Available online at www.sciencedirect.com
SCIENCE DIRECT®
Marine Geology 204 (2004) 91–127
MARINE GEOLOGY
INTERNATIONAL JOURNAL OF MARINE GEOLOGY, GEOCHEMISTRY AND GEOPHYSICS
www.elsevier.com/locate/margeo

Magnetostratigraphic calibration of Eocene–Oligocene dinoflagellate cyst biostratigraphy from the Norwegian–Greenland Sea[1]

James S. Eldrett[a], Ian C. Harding[a,*], John V. Firth[b], Andrew P. Roberts[a]

[a] *School of Ocean and Earth Science, Southampton Oceanography Centre, University of Southampton, European Way, Southampton SO14 3ZH, UK*
[b] *Ocean Drilling Program, 1000 Discovery Drive, College Station, TX 77845-3469, USA*

Received 1 November 2002; received in revised form 30 October 2003; accepted 17 November 2003

Abstract

The presence of abundant age-diagnostic dinoflagellate cysts in Ocean Drilling Program (ODP) Hole 913B (Leg 151), Deep Sea Drilling Project Hole 338 (Leg 38) and ODP Hole 643A (Leg 104) has enabled the development of a new biostratigraphy for the Eocene–Oligocene interval in the Norwegian–Greenland Sea. This development is important because the calcareous microfossils usually used for biostratigraphy in this age interval are generally absent in high latitude sediments as a result of dissolution. In parallel with this biostratigraphic analysis, we developed a magnetic reversal stratigraphy for these Norwegian–Greenland Sea sequences. This has allowed independent age determination and has enabled the dinocyst biostratigraphy to be firmly tied into the global geomagnetic polarity timescale (GPTS). The relatively high resolution of this study has enabled identification of dinoflagellate cyst assemblages that have affinities with those from the North Sea and the North Atlantic, which allows regional correlation. Correlation of each site with the GPTS has also allowed comparison of the stratigraphic record preserved in each drill-hole. Hole 913B is the most complete and is the best-preserved record of the Eocene and Oligocene in the Northern Hemisphere high latitudes, and can serve as a reference section for palaeoenvironmental reconstructions of this age interval.

Keywords: Eocene; Oligocene; dinoflagellate cysts; magnetobiostratigraphy; biostratigraphy; Norwegian–Greenland Sea

1. Introduction

The Eocene–Oligocene interval was a critical phase in Earth history, marking a major climatic transition from greenhouse conditions in the Cretaceous to icehouse conditions in the Cenozoic. Stable oxygen isotope data indicate that, after the late Palaeocene–early Eocene thermal maximum, a long-term cooling trend began at about 52 Ma (Shackleton and Kennett, 1975; Miller et al., 1987; Prentice and Matthews, 1988; Zachos et al., 1994, 2001), with several distinct cooling

[1] Supplementary data associated with this article can be found at doi:10.1016/S0025-3227(03)00357-8

* Corresponding author. Tel.: +44-23-80592071; Fax: +44-23-80593052.
E-mail address: ich@soc.soton.ac.uk (I.C. Harding).

0025-3227/03/$ – see front matter © 2003 Elsevier B.V. All rights reserved.
doi:10.1016/S0025-3227(03)00357-8

events throughout the Eocene culminating in a permanent drop in oceanic bottom water temperatures at the Eocene–Oligocene boundary (Abreu and Anderson, 1998). In the Norwegian–Greenland Sea, early Cenozoic continental separation of Eurasia from Greenland and the subsequent submergence of land bridges, which acted as important barriers to the exchange of surface and deep waters among the Norwegian–Greenland Sea, the Arctic Ocean and the North Atlantic (Eldholm et al., 1994), resulted in major oceanographic and environmental changes.

Stepwise faunal and floral extinctions were associated with this global cooling and evolving hydrographic regime, as temperature sensitive species were replaced by more tolerant taxa (Molina et al., 1993; Bujak, pers. commun. 2001). Dinoflagellate cysts (dinocysts), in particular, are abundant and are extremely diverse throughout the Eocene sequences of the Norwegian–Greenland Sea, and provide a good record of environmental change associated with local tectonic and global climate events.

2. Previous Norwegian–Greenland Sea Palaeogene dinocyst biostratigraphies

Biostratigraphy of high latitude sediments can be difficult because the low-latitude marker species used in many zonation schemes are rarely found in these sediments. In addition, the Eocene–Oligocene (E/O) transition in many high latitude sites is missing in unconformities, which prevents identification of the E/O boundary. The situation has been further complicated by the perceived high level of provincialism of dinocysts in the Norwegian–Greenland Sea, which has made correlation with other sites over wide geographic regions problematical (Damassa and Williams, 1996). The net effect is that the Cenozoic dinocyst biostratigraphy of this region remains in a relatively early stage of development compared to the levels of sophistication achieved for low latitude regions. Previous Palaeogene biostratigraphic dinocyst studies of the Norwegian–Greenland Sea include those of Manum (1976), Manum et al. (1989), Firth (1996), and Poulsen et al. (1996).

Manum (1976) provided the first attempt to develop a dinocyst zonation for this period in the Norwegian–Greenland Sea, based on material from Deep Sea Drilling Project (DSDP) Leg 38, Site 338 (67°47.11′N, 05°23.26′E). This study was limited by low sampling resolution (i.e. one sample every 9 m) and by a rudimentary taxonomy, which was partly a reflection of the exploratory nature of the first DSDP leg in the region (Firth, 1996). Subsequent studies have greatly benefited from better core recovery, enhanced sampling resolution and an improved taxonomic database. However, the later studies of Ocean Drilling Program (ODP) Leg 104, Site 643 (67°47.11′N, 01°02.0′E) by Manum et al. (1989) and Leg 151, Site 913 (75°29.356′N, 6°56.810′W) by Firth (1996) were also limited due to time constraints associated with the ODP publication schedules, which prevented more detailed and quantitative analysis.

Magnetostratigraphic analyses for ODP Legs 104 (Eldholm et al., 1987) and 151 (Myhre et al., 1995) yielded incomplete data, and no palaeomagnetic stratigraphy exists for DSDP Leg 38 (Talwani et al., 1976), which prevents correlation with the geomagnetic polarity timescale (GPTS). In addition, the stratigraphic utility of calcareous and siliceous microfossils, used to constrain the dinocyst biostratigraphy, was also limited by frequent barren intervals that resulted from carbonate and silica dissolution. Therefore, even the synthesised biostratigraphic zonations that resulted from these drilling legs (e.g. Schrader et al., 1976; Goll, 1989; Thiede and Myhre, 1996) have proved problematical in their application.

Gradstein et al. (1992) developed an integrated Cenozoic biostratigraphy for Palaeogene sediments from offshore mid-Norway and the central North Sea, using both dinocysts and foraminifera. However, this scheme has relatively low resolution, with six broad dinocyst zones based on the average last occurrences of dinocyst and foraminiferal taxa. Bujak and Mudge (1994) developed a more detailed Eocene North Sea dinocyst zonation, based on last occurrence and abundance events of dinocyst species. They defined eight Eocene dinocyst zones and twenty-three subzones, which provide a potential source for detailed com-

parison between the North Sea and the Norwegian–Greenland Sea. However, the North Sea zonation of Bujak and Mudge (1994), like the previous Norwegian–Greenland Sea dinocyst biostratigraphies, is not directly calibrated to the GPTS nor to the standard calcareous microplankton zonations as a result of carbonate dissolution in the studied sediments. These authors therefore indirectly calibrated their zonations to the standard calcareous microplankton zonations by comparing their dinocyst successions to those from onshore northwestern Europe where calcareous microfossil age constraints are available.

The relatively high-resolution study presented here has resulted in the identification of abundant age-diagnostic species, which has enabled the development of an improved dinocyst biostratigraphy for this region. Taxonomic advances over the last decade, including discovery of new taxa from the North Sea (Bujak, 1994), have helped to increase the biostratigraphic resolution of our study. Moreover, we also present a new magnetic reversal stratigraphy for the Norwegian–Greenland Sea, which provides the first opportunity to tie the dinocyst biostratigraphy to the GPTS.

3. Materials and methods

3.1. Palynological methods

Dinocysts were counted from approximately 250 palynological slides (average of one sample per ~2.5 m) from ODP holes 913B and 643A and from DSDP Hole 338 in the Norwegian–Greenland Sea (Fig. 1). One of us (J.S.E.) obtained 122 processed samples from Hole 913B (via J.V.F.), which had been subjected to standard palynological preparation techniques (Firth, 1996). Slides from Hole 643A, which had been processed using the method outlined by Manum et al. (1989), were reviewed (by J.S.E.) at the University of Oslo. Additional samples from holes 913B and 338 were processed at the School of Ocean and Earth Science (SOES), University of Southampton, using the standard palynological techniques outlined below.

Samples were demineralised using cold hydrochloric (30% HCl) and hydrofluoric (60% HF) acids. *Lycopodium* spore tablets were added according to the method of Stockmarr (1971) to facilitate the estimation of cyst concentrations. For some samples (~30), one or another of the following procedures were employed. Concentrated nitric acid (70% HNO_3) was employed for oxidation purposes; a tuneable ultrasonic probe was used to break up and remove amorphous organic matter (AOM) from AOM-rich samples, and heavy liquid separation (sodium polytungstate, sp. gr. = 2) was used to remove heavy minerals in samples containing higher concentrations of heavy minerals. Ten-micron sieves were used to concentrate the remaining residues, which were then air-dried on coverslips and mounted on slides using Elvacite. We have used the taxonomic nomenclature of Williams et al. (1998) and the timescales of Berggren et al. (1995) and Cande and Kent (1995) in this study.

Slides were scanned under a stereo-binocular microscope and counting continued until approximately 300 particles had been counted for quantitative analysis. The entire slide was then scanned in order to identify any other diagnostic species that were present in the assemblage. A few samples (~55) were found to contain rather sparse assemblages of dinocysts, in which case the entire slide was counted even when there were fewer than 300 specimens. Only presence–absence data were collected from Site 643A, and each entire slide was scanned to ensure that all species present were identified.

Reworking may be a problem when identifying species range tops, particularly in deep-sea drillholes (i.e. 913B), as dinocysts may be transported from the shelf and subsequently re-deposited in more distal environments (Dale, 1996). Low species abundance, which characterises deep-sea dinocyst assemblages, makes the identification of range tops and the possibility of reworking in Hole 913B difficult. Therefore, species range tops were identified by the occurrence of two or more specimens in a sample. Care was taken only to count unbroken specimens; furthermore, the samples in which these specimens occurred showed no other evidence of reworking (e.g. the occurrence of Cretaceous palynomorphs; see

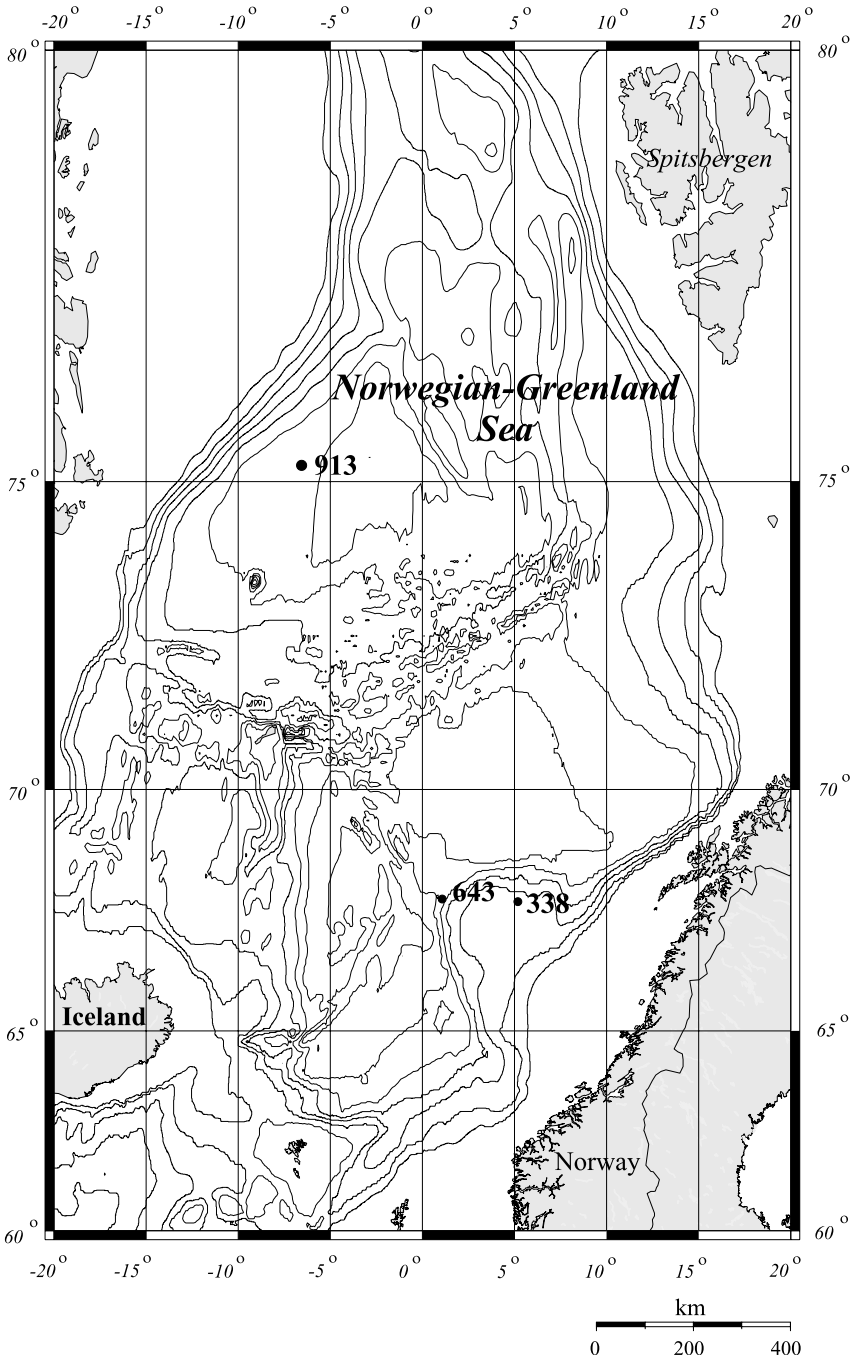

Fig. 1. Map of the Norwegian–Greenland Sea with the locations of sites used in this study: Site 913 (ODP Leg 151), Site 338 (DSDP Leg 38) and Site 643 (ODP Leg 104). Bathymetric contour interval is 500 metres.

Firth, 1996). In addition, species ranges occurred consistently in the same stratigraphic order when compared to adjacent regions (i.e. North Sea; Bujak and Mudge, 1994), which suggests that reworking of range tops is not a significant problem in the studied drill-holes from the Norwegian–Greenland Sea.

3.2. Palaeomagnetic methods

Approximately 500 palaeomagnetic samples were obtained from holes 913B, 338 and 643A, with a sampling resolution of between two and three samples per core section (i.e. one sample every 50–70 cm). Palaeomagnetic measurements were made on discrete samples (7 cm^3 cubes) with a 2-G Enterprises narrow-access pass-through cryogenic magnetometer equipped with high-resolution pick-up coils. All measurements were made in the magnetically shielded palaeomagnetic laboratory at the SOES. The natural remanent magnetisation (NRM) of the samples was subjected to stepwise alternating field (AF) demagnetisation at peak alternating fields of 5, 10, 15, 20, 25, 30, 35, 40, 50, 60, 70, 80, 90, and 100 mT using an AF demagnetiser that is configured in-line with the cryogenic magnetometer. The stability of the NRM was investigated by inspection of vector component plots. If the magnetisation of the sediment decayed to the origin along a straight path, the characteristic remanent magnetisation (ChRM) was calculated using principal component analysis (PCA) with a minimum of four data points (Kirschvink, 1980). The quality of fit of the best-fit line to the selected demagnetisation steps was quantified by determining the maximum angular deviation (MAD) for each measured sample (Kirschvink, 1980). A minimum of four data points was used for PCA, and samples with MAD values $>15°$ were not considered when constructing the magnetic polarity stratigraphy. The studied cores were not azimuthally oriented, however. At the high latitude of the studied sites, the ambient geomagnetic field is dominated by a near-vertical component, which makes it possible to uniquely determine the polarity using the palaeomagnetic inclination alone, without azimuthal orientation of the cores. However, ODP cores can sometimes be dominated by a near-vertical drilling-induced overprint (e.g. Roberts et al., 1996; Fuller et al., 1998; Acton et al., 2002) and it can be difficult to discriminate the ChRM component from the drilling-induced overprint. In such cases, a conservative interpretation was employed and samples suspected of a drilling-induced remagnetisation were excluded from further analysis. Magnetic polarity zones were identified on the basis of two or more samples of a single polarity.

Thermal demagnetisation of an isothermal remanent magnetisation (IRM) was performed on a representative set of samples from different lithologies in the studied holes. IRMs were imparted using an inducing field of 0.9 T. Thermal demagnetisation was done at temperatures of 50, 100, 150, 200, 250, 300, 350, 400, 450, 500, 550, and 580°C.

4. Results

4.1. Palynological results

The present study has resulted in the recovery of an extremely diverse dinocyst assemblage, with over 250 taxa identified, many of which can be used to correlate both between holes and with adjacent sedimentary basins (see background dataset[1]). The main dinocyst datum events identified at each hole are summarised in Table 1.

4.2. Palaeomagnetic behaviour

A near-vertical, normal polarity remanence component, which can be interpreted as a drilling-induced overprint, affects most samples. This overprint is usually removed at peak fields of 5–10 mT (Fig. 2). AF demagnetisation between 10 and 50 mT enabled separation of the stable remanence directions from the near-vertical drilling-induced overprint for the majority of samples (e.g. Fig. 2a–d). Some samples contained higher coercivity components and required AF demagnetisation up

[1] See online version of this article.

Table 1
Dinocyst datum events from the Eocene–Oligocene of the Norwegian–Greenland Sea

Event	Key	Hole 913B			Hole 643A			Hole 338			CSRS 3		Published literature
		Depth (mbsf)	Chron	Age (Ma)	Depth (mbsf)	Chron	Age (Ma)	Depth (mbsf)	Chron	Age (Ma)	Chron	Age (Ma)	Age (Ma)
LO *Adnatosphaeridium vittatum*	Av	623.03	C21n	46.5	540.40	C20r–C21n	45.5–47.0	288.33	C21n	46.5	C21n	46.6	46.1[k]
LO *Areoligera medusettiformis*	Am	684.73	C21r	48.9	540.40	C21n	47.0	287.35	C20r	45.6	C21n	46.7	48.0[j]
FO *Areoligera? semicirculata*	As	–	–	–	488.08	C18n.1n	38.5	–	–	–	C18n.1n	38.5	33.7[d]
LO *Areoligera tauloma*	At	–	–	–	510.00	C19r–C19n	41.8–41.3	260.60	C18n.2n	39.8	C18r	40.2	40.3[k]
LO *Areosphaeridium diktyoplokum*	Ad	452.80	C13n	33.3	481.00	No data	–	253.84	C13n	33.0	C13n	33.4	33.7[k]–33.3[m]
FO *Areosphaeridium ebdonii*	Ae	655.73	C21r	47.8	541.90	C21r–C21n	48.0–47.2	293.38	C21r	48.9	C21r–C21n	48.0	49.9[j]
LO *Areosphaeridium ebdonii*		582.94	C20r	45.2	524.20	C20n	43.5	261.25	C18r	40.3	C20n	43.5	45.2[a]
LO *Areosphaeridium michoudii*	Ami	464.30	C16n.1n	35.3	481.00	No data	–	260.60	No data	–	C16n.1n	35.4	35.4[a]
LO *Batiacasphaera compta*	Bc	452.80	C13n	33.3	–	–	–	453.84	C13n	33.0	C13n	33.4	33.7[j]
FO *Cerebrocysta magna*	Cm	675.13	C21r	48.5	556.21	C21r	49.0	293.38	C21r	48.9	C21r	48.6	51.0[j]
LO *Cerebrocysta magna*		611.94	C20r	46.1	540.40	C20r–C21n	45.5–47.0	286.74	C20r	45.6	C20r	46.2	46.3[a]
LO *Cereodinium depressum*	Cd	589.57	C20r	45.4	–	–	–	277.16	C19r	42.3	C20r	44.9	45.2[a]
LO *Charlesdowniea tenuivirgula*	Ct	578.43	C20r	44.2	–	–	–	262.00	C18r	40.3	–	–	43.7[j]
LO *Charlesdowniea columna*	Cc	703.73	C22n	48.8–49.2	–	–	–	295.52	C21r	48.9	C22n	49.0	50.1[a]
FO *Chiropteridium galea*	Cg	453.59	C13n	33.2	464.70	C13n–C13r	33.1–33.6	253.84	C12r–C13n	33.2	C13n–C13r	33.2–33.6	33.5[d]
FO *Chiropteridium lobospinosum*	Cl	453.59	C13n	33.2	464.70	C13n–C13r	33.1–33.6	253.84	C12r–C13n	33.2	C13n–C13r	33.2–33.6	33.5[p]
LO *Cordosphaeridium funiculatum*	Cf	464.30	16n.1n	35.3	–	–	–	257.21	No data	–	16n.1n	35.3	35.0[f]
LO *Diphyes colligerum*	Dc	531.15	C19n	41.3	507.00	C19n	41.4	257.75	C18n.1r	39.7	C19n	41.3	41.3[k]
FO *Diphyes ficusoides*	Df	703.73	C22n	49.5	–	–	–	320.40	C22n	49.5	C22n	49.6	50.2[j]
LO *Diphyes ficusoides*		598.28	C20r	45.4	540.40	C20r–C21n	45.5–47.0	287.35	C20r	45.6	C20r	45.4	45.8[a]
FO *Distatodinium ellipticum*	De	549.40	C20n	42.1	507.00	C19n	41.4	268.41	C19n	41.4	C19r	41.7	41.4[j]
FO *Dracodinium pachydermum*	Dp	709.56	C22n	49.7	–	–	–	320.40	C22n	49.5	C22n	49.7	50.7[L]
LO *Dracodinium pachydermum*		630.39	C21n	46.8	546.15	C21n	47.2	289.75	C21n	47.3	C21n	47.1	48.0[k]
LO *Eatonicysta ursulae*	Eu	661.54	C21r	48.5	556.20	C21r	48.5	291.91	C21r	49.0	C21r	48.6	49.0[k]–48.5[b]
FO *Enneadocysta arcuata*	Ea	550.90	C19r	42.3	524.20	C20n	43.4	268.41	C19n	41.4	C19r	41.7	47.9[j]
LO *Glaphyrocysta ordinata*	Go	510.89	C18r	39.9	524.20	C20n	43.4	258.30	C18n.2n	39.6	–	–	46.3[f]
FO *Heteraulacacysta porosa*	Hp	579.91	C20r	45.3	530.80	C20r	45.3	268.41	C19n	41.2	C20r	44.8	41.0[g]
LO *Heteraulacacysta porosa*		474.20	C16r	36.4	478.00	No data	–	257.75	No data	–	C16r	36.4	37.0[a]
LO *Hystrichosphaeropsis costae*	Hc	625.94	C21n	46.7	–	–	–	290.65	C21n	47.4	C21n	46.7	47.1[a]
LO *Hystrichostrogylon clausenii*	Hcl	–	–	–	–	–	–	288.90	C21n	47.1	C21n	47.1	47.0[a]
LO *Hystrichosphaeridium tubiferum*	Ht	602.78	C20r	45.8	–	–	–	–	–	–	C20r	45.8	47.1[a]
LO *Lentinia wetzelii*	Lw	601.28	C20r	45.5	–	–	–	–	–	–	C20r	45.5	–
LO *Melitasphaeridium pseudorecurvatum*	Mp	463.07	C15r	35.1	478.00	C15n	34.6	257.21	C13r	33.6	C15n	34.7	34.5[m]–33.0[h]
FO *Phthanoperidinium distinctum*	Pd	579.91	C20r	44.2	518.20	C20n	43.9	267.67	C19r–C19n	41.3	C20n	43.2	44.6[L]
LO *Phthanoperidinium distinctum*		483.60	C17n.2n	37.6	479.50	C17n	38.0	260.60	C18.2n	39.8	C17n.2n	37.7	42.0[k]
■■*Phthanoperidinium geminatum*	Pg	568.73	C20n	43.6	513.00	C20n	42.7	278.07	C19r–C20n	42.4	C20n	42.9	–
■*Phthanoperidinium geminatum*		531.15	C19n	41.3	507.00	C19n	41.4	257.21	C18n.1r	39.7	C19n	41.3	–
FO *Phthanoperidinium regalis–clithridium*	Pc	602.78	C20r	45.8	540.40	C21n	46.9	287.35	C20r–C21n	46.2	C20r	46.1	46.8[j]
LO *Phthanoperidinium regalis–clithridium*		582.94	C20r	45.2	530.80	C20r	44.2	278.59	C19r–C20n	42.4	C20r	44.6	45.2[k]
FO *Reticulatosphaera actinocoronata*	Ra	464.30	C15r	35.3	482.50	No data	–	–	–	–	C15r	35.3	35.1[f]
FO *Rhombodinium rhomboideum*	Rr	513.84	C18n.2n	40.1	–	–	–	263.90	C18n.2n	39.9	C18n.2n	39.9	44.2[L]
LO *Rhombodinium rhomboideum*		500.65	C18n.1n	39.5	–	–	–	263.40	C18n.1r	39.8	C18n.1r	39.6	41.3[k]
LO *Rottnestia borussica*	Rb	502.15	C18n.1n	39.1	507.00	C18.2n–C19n	39.7–41.4	257.21	C18n.1r	39.6	C18n.1r	39.6	37.8[a]
FO *Spiniferites* sp. 1	Ssp1	453.59	No Data	33.3	463.20	C13n	33.0	–	–	–	C13n–C13r	33.2–33.6	31.5[c]
LO *Spiniferites* sp. 1		438.30	C12n	30.9	458.70	C12r	32.0	–	–	–	C12r	31.0	31.3[c]
FO *Svalbardella cooksoniae*	Sc	541.34	C19r	42.0	507.00	C19r	41.4	268.41	C19r	42.2	C19r	41.9	–
LO *Svalbardella cooksoniae*		463.07	C15r	35.1	468.40	C13r	33.6	257.21	C13r	33.6	C13r	33.6	32.8[f]–30.5[c]
FO *Wetzeliella gochtii*	Wg	453.59	C13n	33.3	478.00	C15n	34.6	–	–	–	C13n–C13r	33.2–33.6	32.8[f]
FO *Wetzeliella ovalis*	Wo	578.43	C20r	44.1	540.40	C21n	46.9	267.67	C19n	41.3	C20r	44.3	44.2[f]
LO *Wetzeliella ovalis*		573.27	C20r	43.9	507.00	C19n	41.4	260.60	C18n.2n	39.9	C18r	40.2	41.3[a]

Abbreviations used in Figs. 5–10 and 12 are given in the column labelled 'Key'. Superscripted letters refer to references from which ages for first occurrence (FO) and last occurrence (LO) datum events are taken: a = Bujak (1994), b = Williams and Bujak (1985), c = Williams and Manum (1999), d = Stover and Hardenbol (1994), e = Köthe (1990), f = Williams et al. (2001), g = Bujak (1980), h = Williams et al. (1993), j = Williams et al. (1999), k = Bujak and Mudge (1994), L = Mudge and Bujak (1996), m = Brinkhuis and Biffi (1993), Powell (1992). mbsf = metres below sea floor.

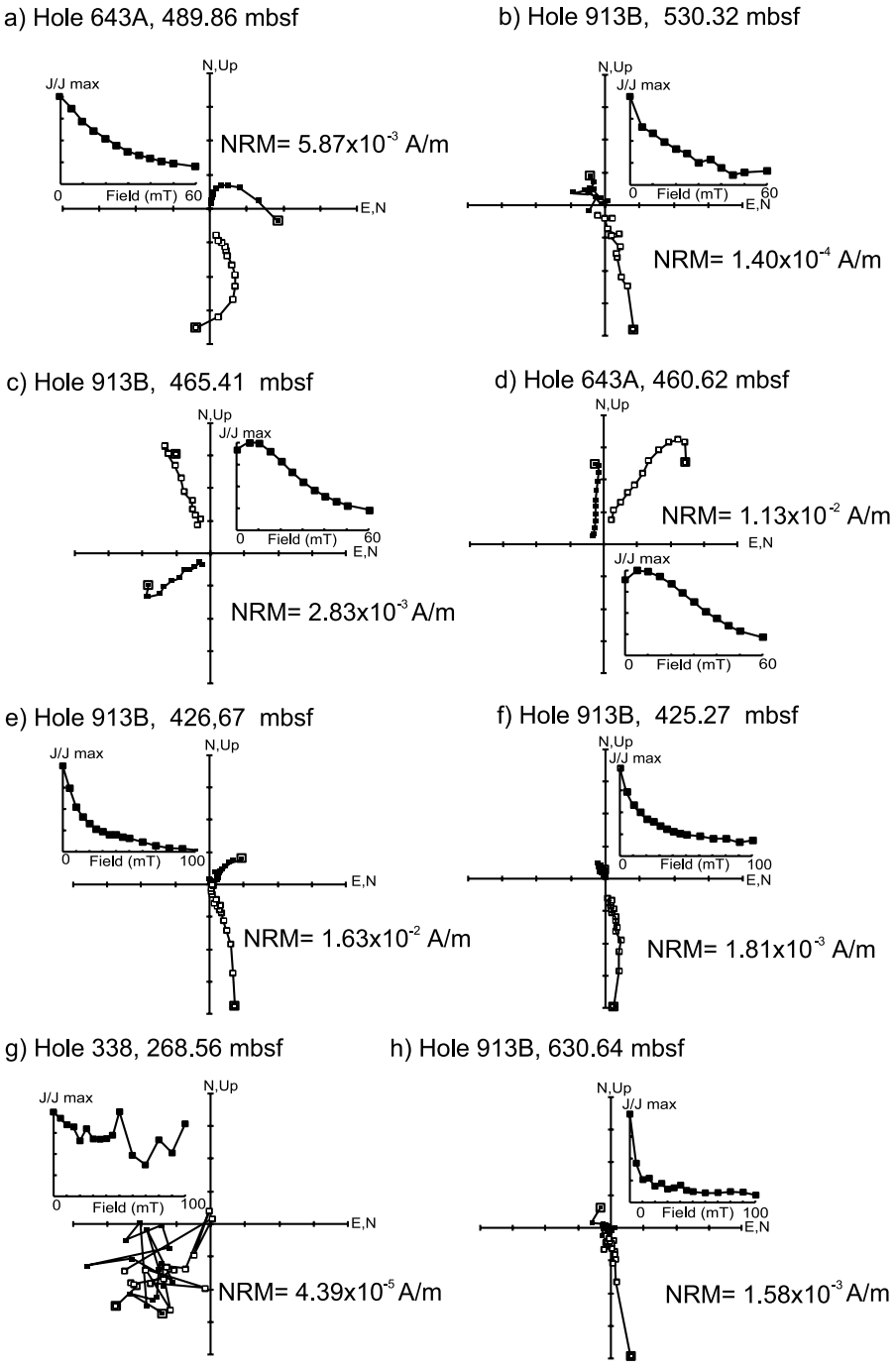

Fig. 2. Vector component diagrams of demagnetisation behaviour for representative samples from holes 913B, 338 and 643A. (a,b) Demagnetised to 60 mT, stable behaviour, normal polarity. (c,d) Demagnetised to 60 mT, stable behaviour, reversed polarity. (e,f) Demagnetised to 100 mT, stable behaviour, normal polarity. (g) Unstable magnetisation. (h) Dominantly drilling-induced overprint.

to 100 mT in order to isolate the ChRM direction (e.g. Fig. 2e,f).

For 88% of the samples, stable palaeomagnetic behaviour was evident in the vector component diagrams with ChRM directions generally tending toward the origin of the diagrams. ChRM directions could not be obtained for 12% of the samples, either because the sample was unstably magnetised (Fig. 2g) or because of a near-vertical drilling-induced remagnetisation (Fig. 2h). Most of these samples were weakly magnetised and exhibited no systematic behaviour during AF demagnetisation (e.g. Fig. 2g). These samples were mainly from holes 338 and 913B and are from biosiliceous ooze intervals. The weak magnetisations in the biosiliceous ooze intervals have several possible causes including dilution of terrigenous material by non-magnetic biogenic silica, diagenetic dissolution resulting from microbial degradation of elevated organic carbon contents (e.g. Karlin and Levi, 1983), and diagenetic dissolution resulting from likely elevated porewater silica concentrations (e.g. Florindo et al., 2003). Despite the weak magnetisations in these biosiliceous ooze intervals it was still possible to obtain reliable palaeomagnetic directions for a majority of samples, which represents a major refinement of previous shipboard palaeomagnetic studies and has enabled the development of useful magnetic polarity stratigraphies for holes 913B, 338 and 643A.

4.3. Rock magnetism

In each case, regardless of lithology, the IRM decreases to near-zero values at 580°C (Fig. 3), which suggests that magnetite is the dominant magnetic mineral in the studied sediments. The

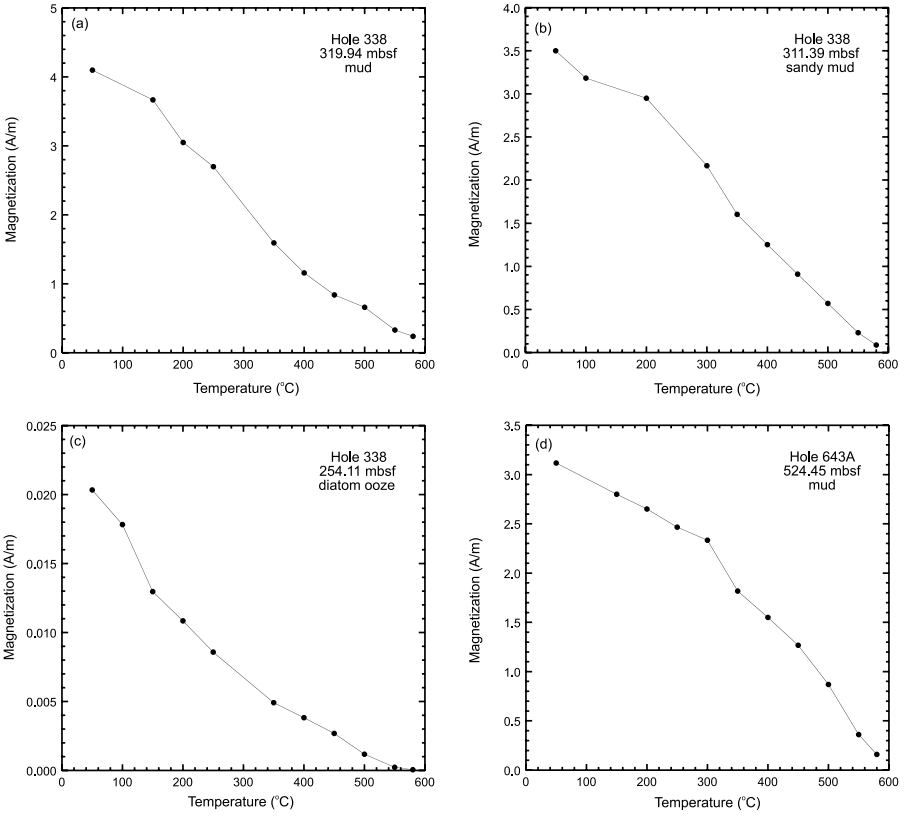

Fig. 3. Results of thermal demagnetisation of an isothermal remanent magnetisation for representative lithologies for the studied holes. In each case, the magnetisation decreases to near-zero values near 580°C, which indicates that magnetite is the dominant magnetic mineral in the studied sediments.

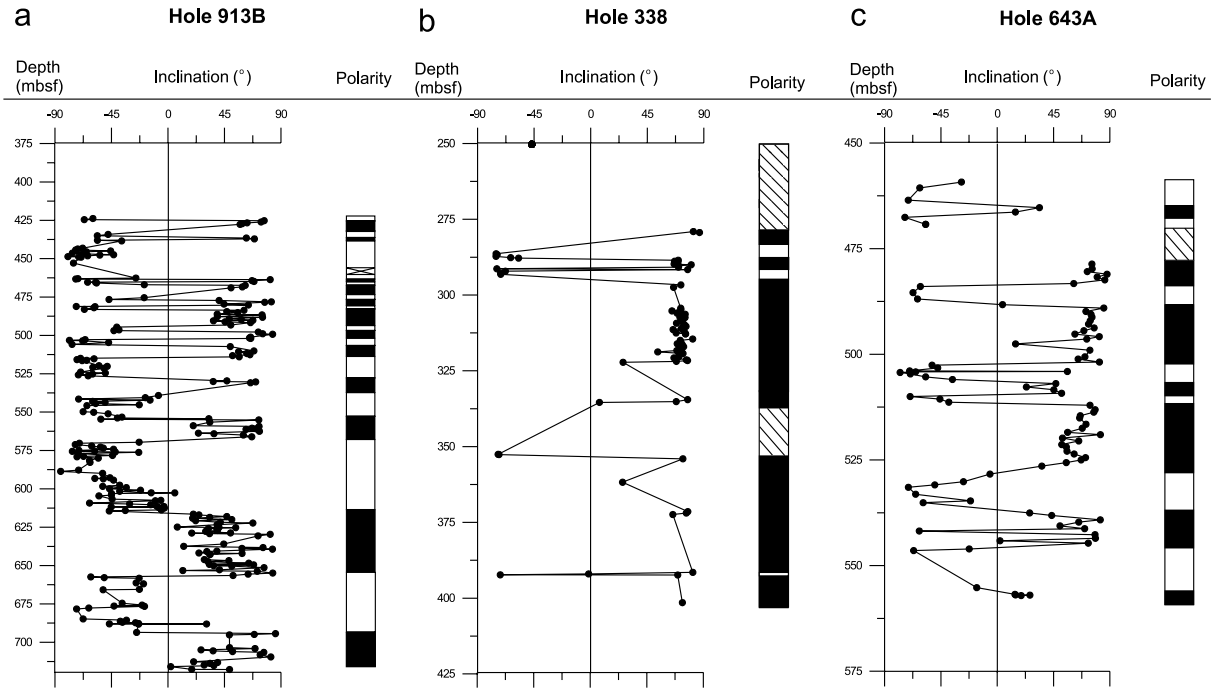

Fig. 4. For each studied hole, the magnetic reversal stratigraphies are illustrated alongside the down-core variation of inclination of characteristic remanent magnetisation following stepwise alternating field demagnetisation. Magnetic polarity reversal stratigraphy: black, normal polarity; white, reversed polarity; hatched, unknown polarity.

magnetisation of the biosiliceous ooze (Fig. 3c) is more than 2 orders of magnitude less than that of the terrigenous lithologies. This suggests that either the elevated organic carbon contents or dissolved silica contents have given rise to diagenetic dissolution of magnetite (e.g. Karlin and Levi, 1983; Florindo et al., 2003). Regardless, it is clear that small concentrations of magnetite have survived (Fig. 3c), which gives rise to a measurable palaeomagnetic signal even in the biosiliceous oozes.

4.4. Magnetic polarity stratigraphy

Previous palaeomagnetic studies in the Norwegian–Greenland Sea for the Eocene–Oligocene interval have not enabled development of robust magnetostratigraphies. It was not possible for Hole 913B because the remanence intensity in weakly magnetised intervals dropped below the noise level of the shipboard cryogenic magnetometer. Shipboard palaeomagnetic analysis for Hole 643A was restricted to the uppermost Quaternary section, and no previous palaeomagnetic studies have been attempted for Hole 338. The higher sensitivity of the cryogenic magnetometer used in the present study (nominal noise level of 10^{-6} A/m) has resulted in successful isolation of the ChRM for most samples and has enabled the development of magnetic reversal stratigraphies for holes 913B, 338 and 643A, as illustrated in Fig. 4. The timescale of Berggren et al. (1995) and Cande and Kent (1995) was used to correlate the magnetic reversal stratigraphies for each hole with the GPTS. Correlation was accomplished by determining the best fit of the reversal stratigraphies with the GPTS for this time period (Figs. 5–7), using the chronostratigraphic control from Firth (1996) as a first constraint for Hole 913B.

4.5. Graphic correlation

Shaw (1964) discussed methods of correlating

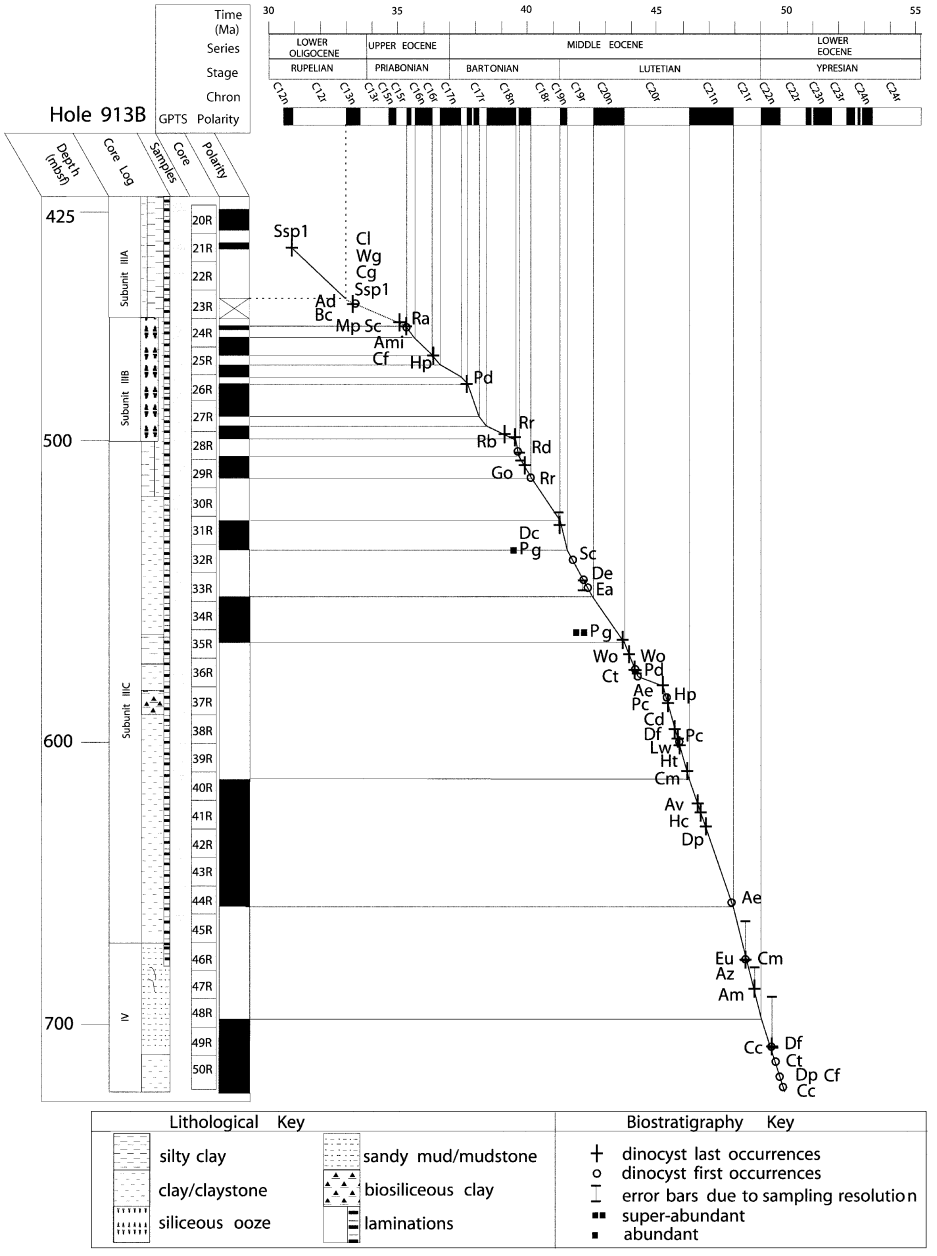

Fig. 5. Age–depth plot for Hole 913B against the GPTS of Cande and Kent (1992, 1995) and Berggren et al. (1995). Magnetic polarity reversal stratigraphy symbols are defined in Fig. 4. Line of correlation: solid line, correlation is unambiguous; dashed line, correlation is inferred. Dinocyst species abbreviations are defined in Table 1.

geological sequences and his technique, now known as graphic correlation, has been widely employed for resolving geological problems (e.g. Dowsett, 1989; Neal et al., 1994; Armstrong, 1999). Graphic correlation is now well established (Miller, 1977; Edwards, 1984; Carney and Pierce, 1995) and is employed here.

Graphic correlation was performed using the new palaeomagnetic stratigraphies and the first and last occurrences (FO and LO, respectively)

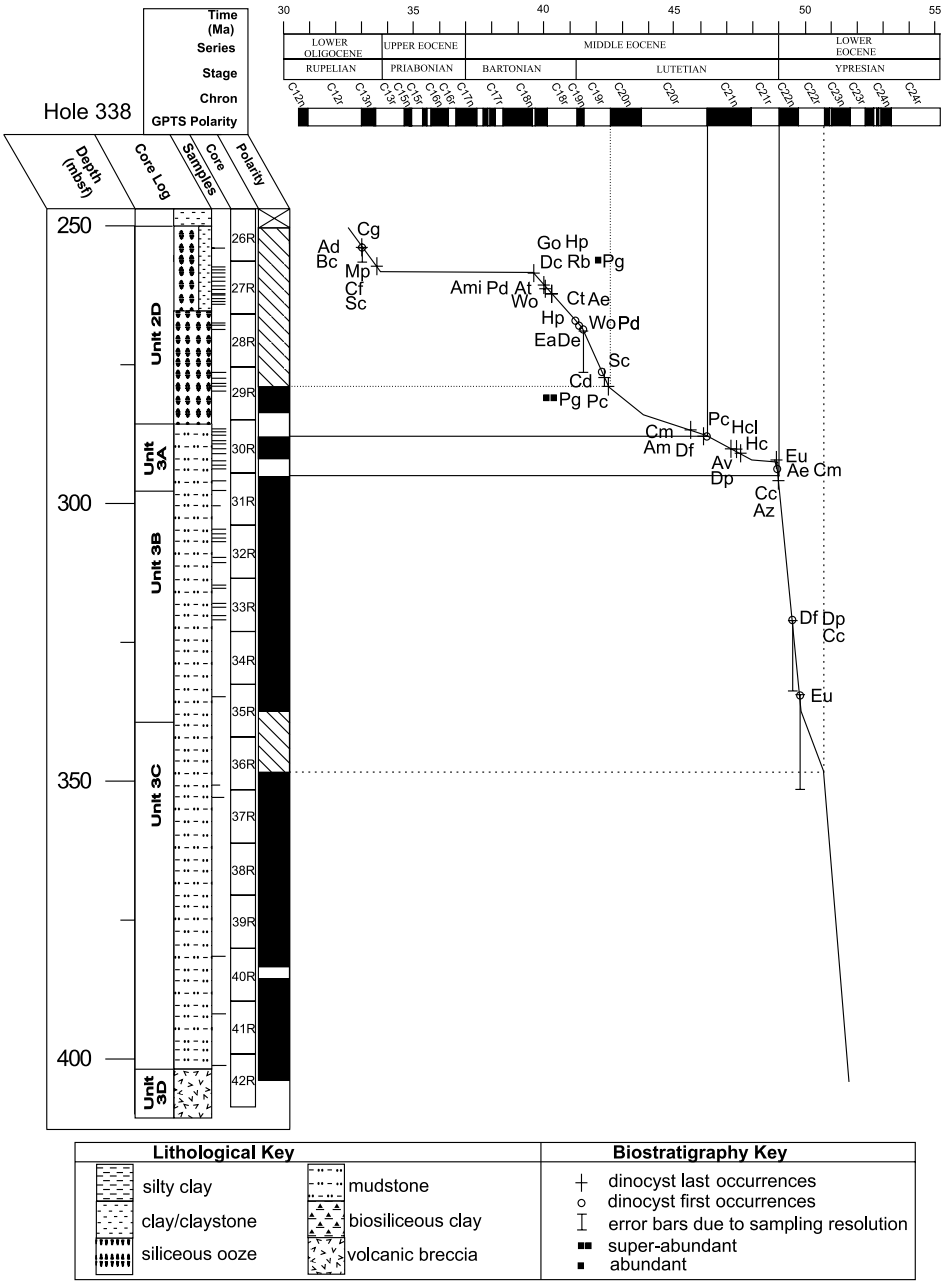

Fig. 6. Age–depth plot for Hole 338 against the GPTS of Cande and Kent (1992, 1995) and Berggren et al. (1995). Magnetic polarity reversal stratigraphy symbols are defined in Fig. 4. Line of correlation: solid line, correlation is unambiguous; dashed line, correlation is inferred. Dinocyst species abbreviations are defined in Table 1.

of dinocyst taxa in the measured sections of holes 913B, 338 and 643A. Hole 913B was used as a standard reference section (SRS) because it has the most complete sedimentary record, the greatest sampling density and the most FO/LO events. Hole 338 was then plotted against the SRS and time equivalent levels were correlated (Fig. 8). Conventions have been maintained

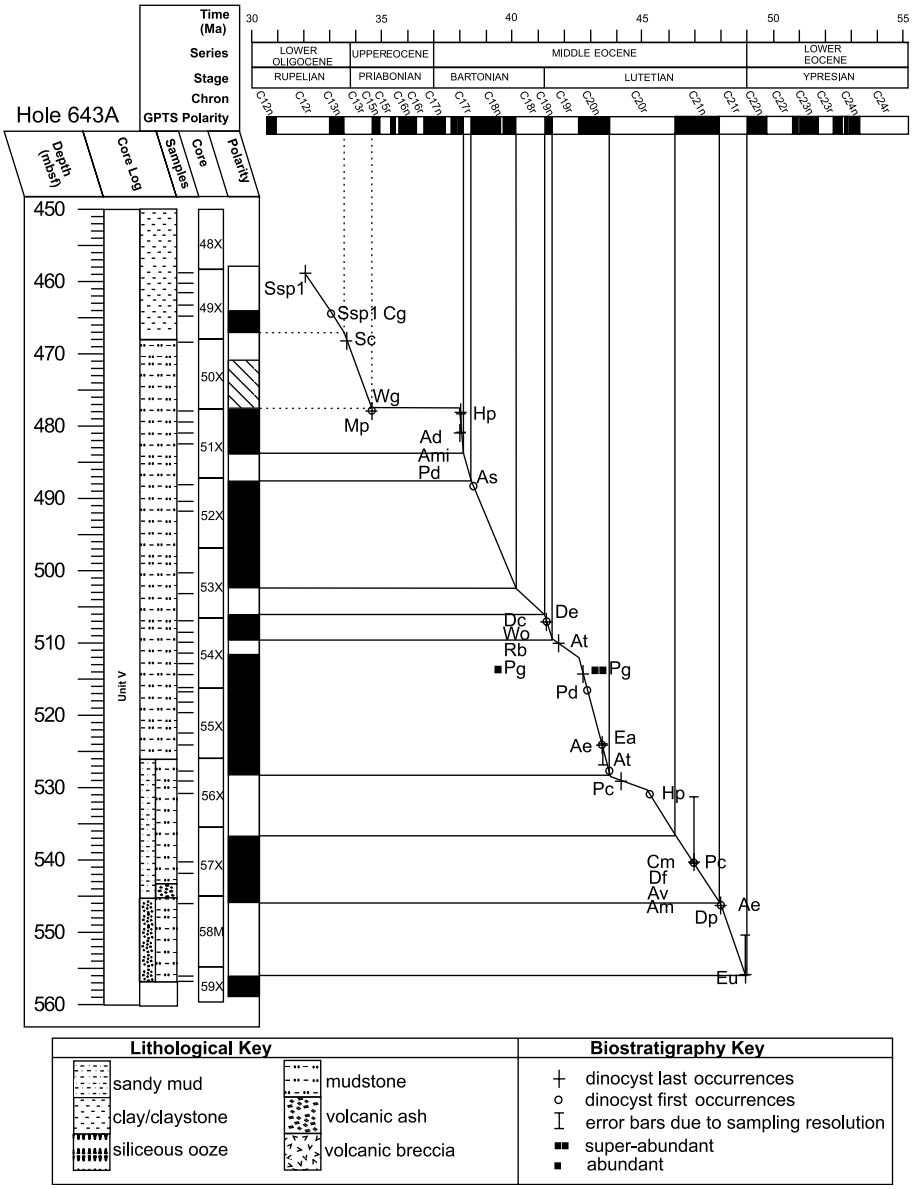

Fig. 7. Age–depth plot for Hole 643A against the GPTS of Cande and Kent (1992, 1995) and Berggren et al. (1995). Magnetic polarity reversal stratigraphy symbols are defined in Fig. 4. Line of correlation: solid line, correlation is unambiguous; dashed line, correlation is inferred. Dinocyst species abbreviations are defined in Table 1.

when plotting different types of data in Figs. 5–10: open circles indicate first occurrences, crosses (+) indicate last occurrences and x's indicate magnetic reversal tie-points. This procedure has resulted in development of a composite standard reference section (CSRS), which is calibrated in composite units (CU). The process of graphic correlation was continued by plotting the data from Hole 643A against the CSRS, and adjusting events as appropriate (Fig. 9). This completed the first round of compositing, resulting in CSRS 1.

After the first round of compositing the procedure was repeated several times in order to reduce

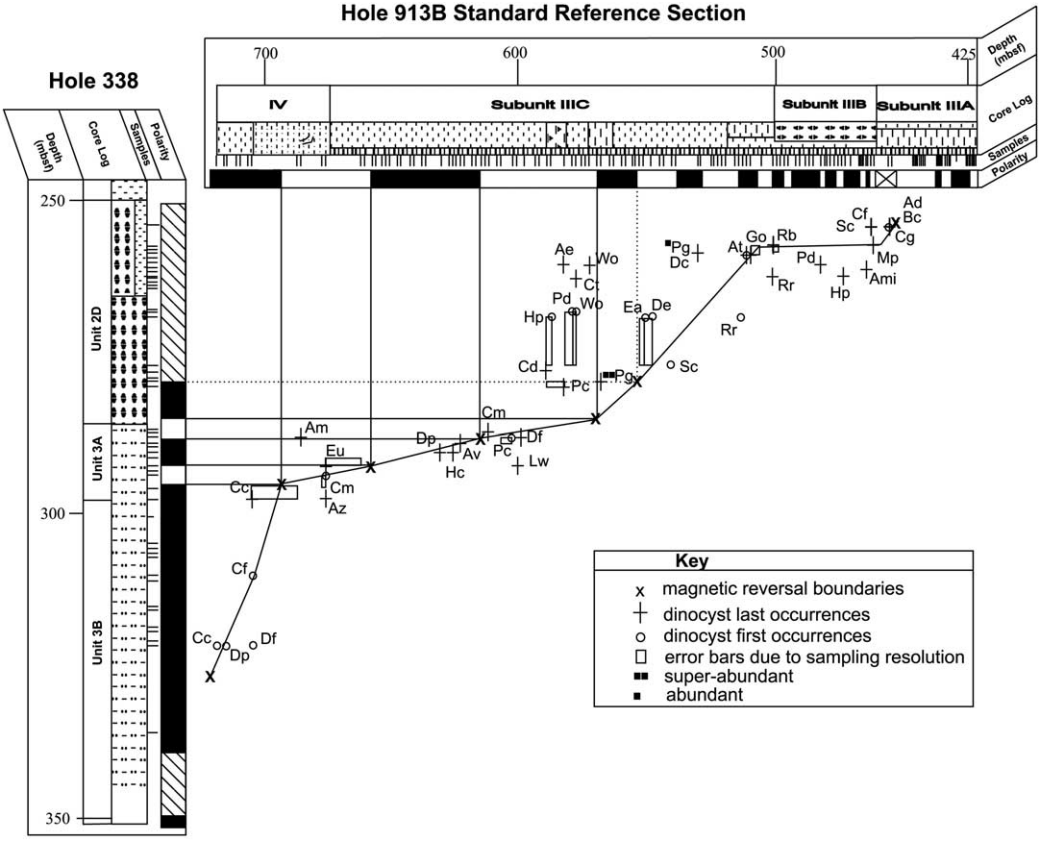

Fig. 8. Graphic correlation of stratigraphic events from Hole 338 displayed against the standard reference section (Hole 913B). Dinocyst species abbreviations are defined in Table 1. Lithological symbols are defined in Fig. 5. The line of correlation represents a best-fit through the calibrated datum events.

the scatter of datum events around the line of correlation. In further rounds, each section was compared in turn with the composite section exclusive of those values in the composite that are derived from the sections being compared. Two further rounds of compositing were performed until the position of events in the CSRS stabilised, resulting in CSRS 3.

5. Magnetostratigraphic calibration of palynological datum events

To calibrate the main datum events against an numerical timescale, CSRS 3 was plotted against the GPTS (Fig. 10). The main datum events from the Norwegian–Greenland Sea that have been calibrated against the GPTS are presented in Fig. 11, and are discussed below in stratigraphic order from oldest to youngest.

FO *Dracodinium pachydermum* (Dp)

Direct calibration: magnetic polarity chronozone: C22n.

Indirect calibration: calcareous nannofossil zone: NP14a; planktonic foraminiferal zone: P9.

Age assignment: 49.7 Ma.

Discussion: in the North Sea, the FO of *Dracodinium pachydermum* was indirectly correlated with NP13 (Bujak and Mudge, 1994; Mudge and Bujak, 1996). Occurrences of *D. pachydermum* have also been recorded in northwestern Europe, where it appears in the standardised Northwest European Zone D9, which is indirectly correlated to

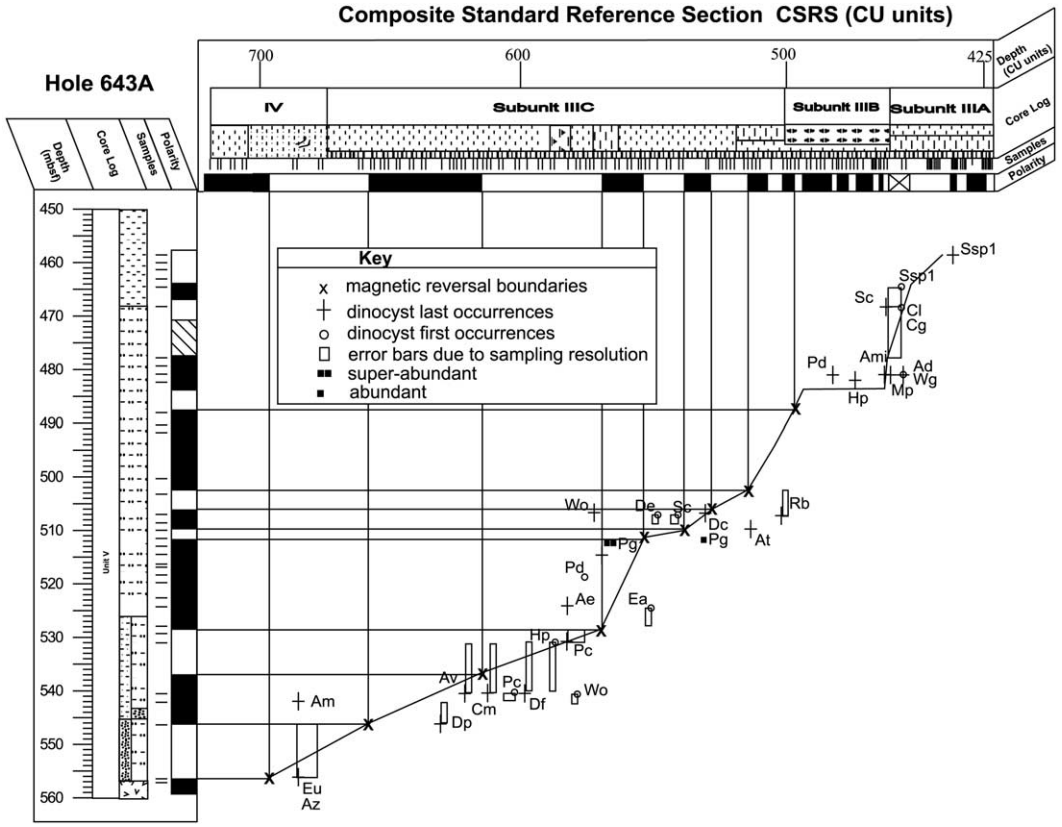

Fig. 9. Graphic correlation of stratigraphic events from Hole 643A displayed against the composite standard reference section (CSRS). Dinocyst species abbreviations are defined in Table 1. Lithological symbols defined in Fig. 5. The line of correlation represents a best-fit through the calibrated datum events.

NP13–NP14 (Costa et al., 1988). In holes 913B and 338 from the Norwegian–Greenland Sea, we correlate the FO of *D. pachydermum* to Chron C22n, which corresponds to NP14a.

FO *Diphyes ficusoides* (Df)

Direct calibration: magnetic polarity chronozone: C22n.

Indirect calibration: calcareous nannofossil zone: NP14a; planktonic foraminiferal zone: P9.

Age assignment: 49.6 Ma.

Discussion: in the North Sea, Mudge and Bujak (1996) recorded the FO of *Diphyes ficusoides* near the base of their E2b Subzone, which is indirectly correlated to NP12. However, the worldwide FO of *D. ficusoides* is correlated with NP13, and is assigned an age of 50.2 Ma (Williams et al., 2001). In the Norwegian–Greenland Sea, the FO of *D. ficusoides* is directly correlated with Chron C22n, with an age (49.6 Ma) that is slightly younger, although better constrained, than that previously proposed (Fig. 11).

LO *Charlesdowniea columna* (Cc)

Direct calibration: magnetic polarity chronozone: top of C22n.

Indirect calibration: calcareous nannofossil zone: NP14a; planktonic foraminiferal zone top of P9.

Age assignment: 49.0 Ma.

Discussion: *Charlesdowniea columna* was first described by Michoux (1988) from southwestern France, in strata assigned to NP13 by Kapellos and Schaub (1975) and Bigg (1982), and has also been documented in lower Eocene sediments from the North Sea (Ioakim, 1979; Bujak and Mudge, 1994). This species was also recorded as *Kisselovia*

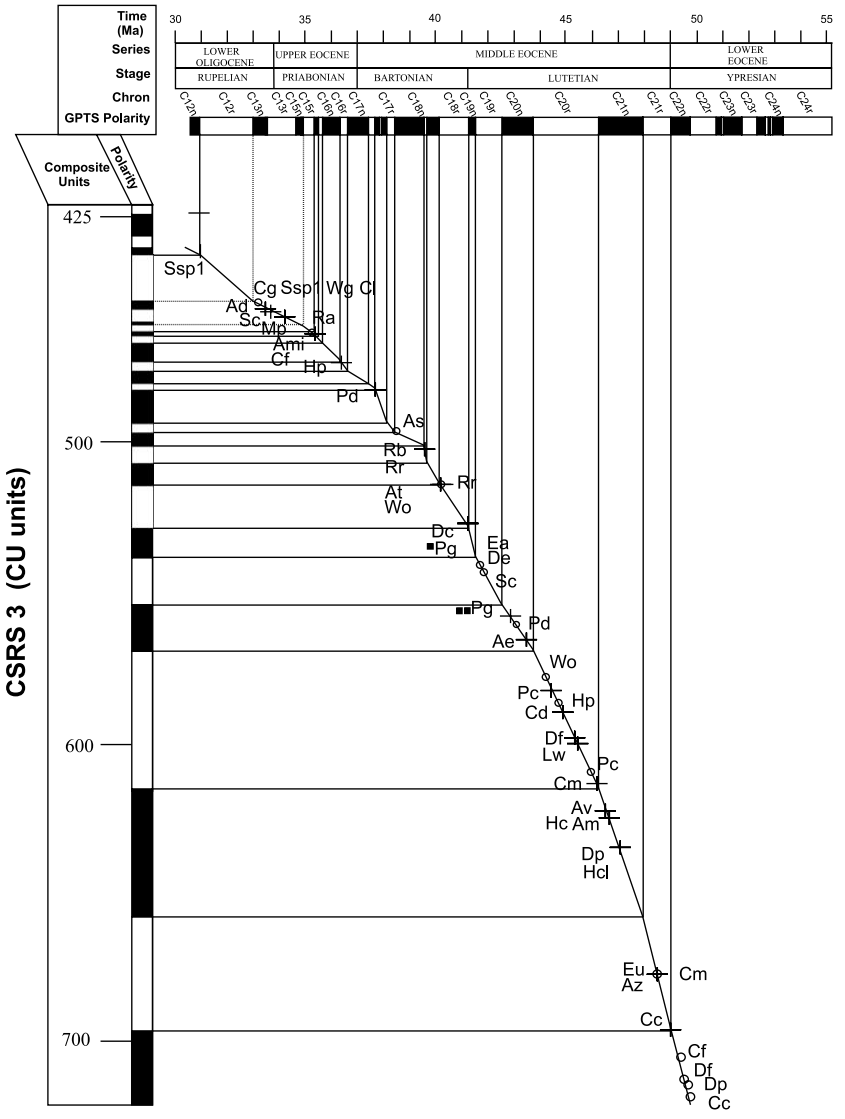

Fig. 10. Graphic correlation diagram (Shaw plot) of the Composite Standard Reference Section after composite round III (CSRS 3) against the GPTS of Cande and Kent (1992, 1995) and Berggren et al. (1995). Magnetic polarity reversal stratigraphy symbols are defined in Fig. 4. Dinocyst species abbreviations are defined in Table 1.

edwardsii in Zone NP13 from the Rockall Plateau (Brown and Downie, 1984) and as *Kisselovia edwardsii* sensu Caro 1979 from the Labrador Sea (Head and Norris, 1989). The LO of *C. columna* (as *Kisselovia* cf. *edwardsii*) has also been recorded between strata assigned to NP12 and NP14 (Heilmann-Clausen and Costa, 1989) in the Heiligen Hafen Formation in the Wursterheide borehole of northwest Germany. The magnetic reversal stratigraphy developed for the Norwegian–Greenland Sea enables direct calibration of the LO of *C. columna* with Chron C22n, giving a later LO for this species in the Norwegian–Greenland Sea than in adjacent basins (Fig. 12).

LO *Eatonicysta ursulae* (Eu)

Direct calibration: magnetic polarity chronozone: C21r.

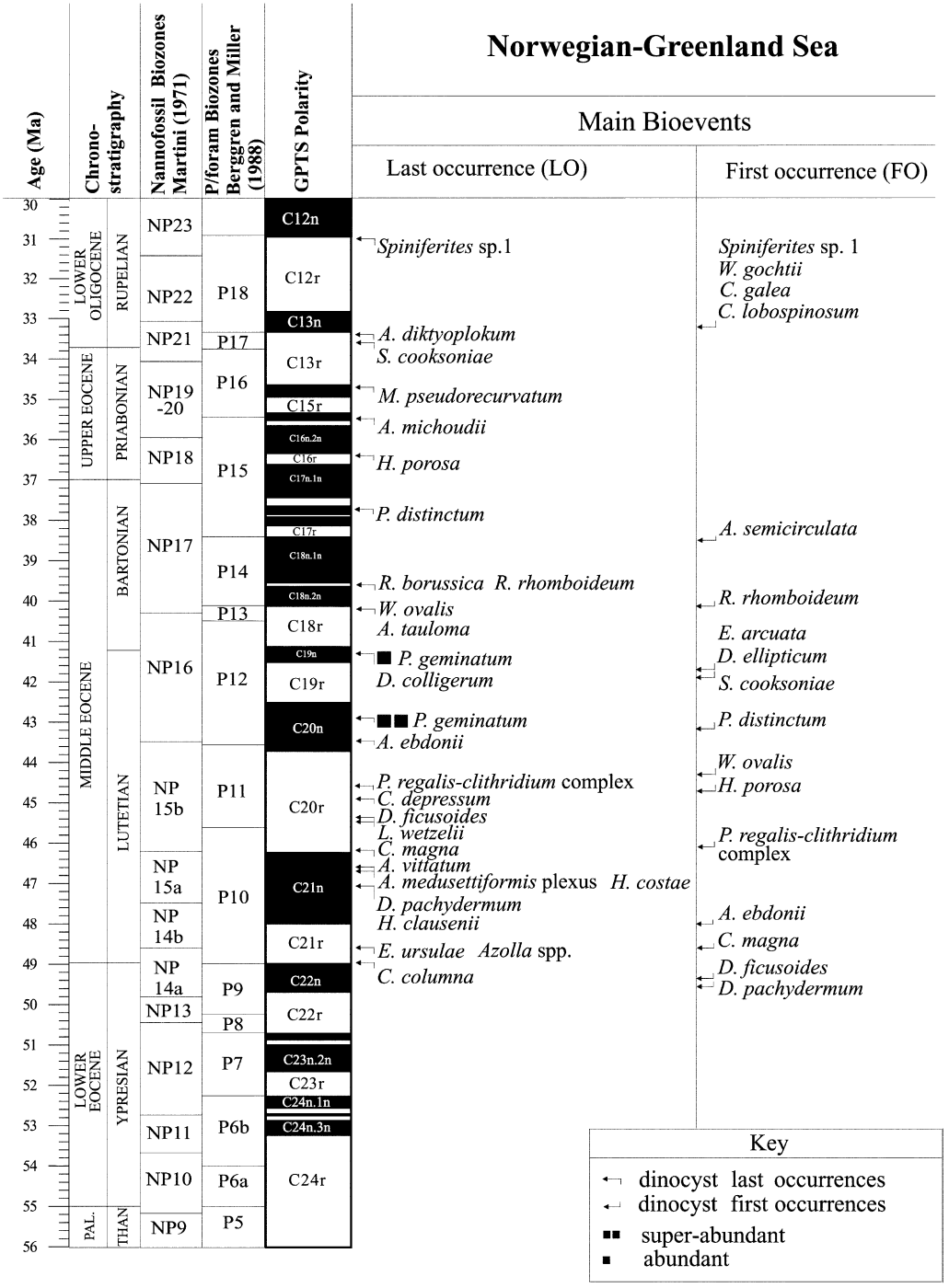

Fig. 11. New magnetobiostratigraphic calibration of the main bioevents for the Norwegian–Greenland Sea, based on the composite section developed from holes 913B, 338 and 643A (CSRS 3).

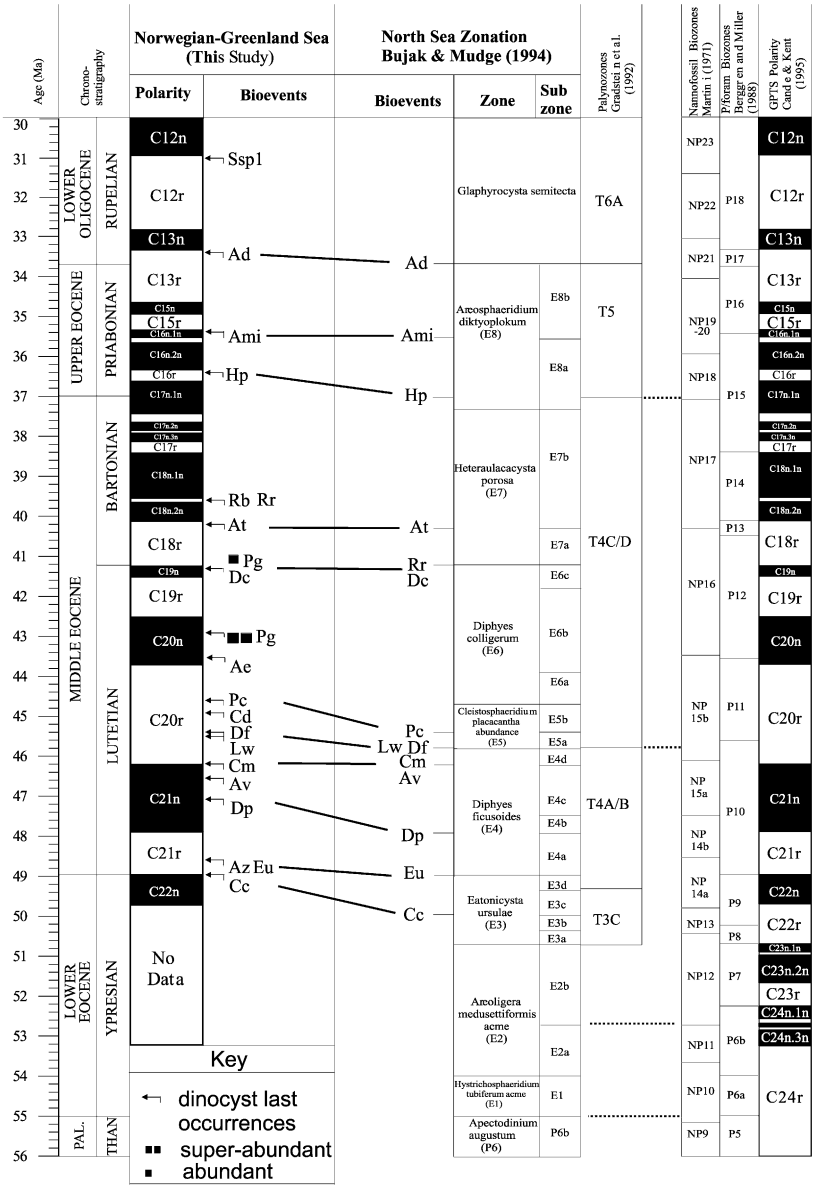

Fig. 12. Correlation of the main dinocyst datum bioevents for the Norwegian–Greenland Sea (this study) with the North Sea (Bujak and Mudge, 1994; Gradstein et al., 1992).

Indirect calibration: calcareous nannofossil zone: top of NP14a; planktonic foraminiferal zone: base of P10.

Age assignment: 48.6 Ma.

Discussion: *Eatonicysta ursulae* has been reported to have a worldwide LO in the Lutetian NP15 nannoplankton biozone (Stover and Williams, 1995). However, in the North Sea, the LO of *E. ursulae* has been correlated with the top of the Ypresian (Harland et al., 1992) and with the lower Lutetian (Gradstein et al., 1992). Bujak and Mudge (1994) assigned the top of their *E. ursulae* Biozone and Subzone to NP14a, with the LO of *E. ursulae* occurring at 49 Ma. The LO of *E. ursulae* has also been documented from several northwestern European onshore sections that

have been assigned to NP14 (Eaton, 1976; De Coninck, 1977; Cepek et al., 1988; Costa et al., 1988; Heilmann-Clausen and Costa, 1989). Our magnetic reversal stratigraphy constrains the LO of *E. ursulae* in the Norwegian–Greenland Sea to Chron C21r (~48.6 Ma). The LO of *E. ursulae* in the Norwegian–Greenland Sea is equivalent to the top of the *Eatonicysta ursulae* Biozone (E3) of the North Sea (Bujak and Mudge, 1994). This biozone corresponds in part with Zone T3C of Gradstein et al. (1992). A slight offset between the two schemes occurs because Gradstein et al. (1992) identified the top of Zone T3C using the top acme of *E. ursulae*, whereas we follow Bujak and Mudge (1994) in using the LO of *E. ursulae* (Fig. 12).

LO *Azolla* spp. (Az)
Direct calibration: magnetic polarity chronozone: C21r.
Indirect calibration: calcareous nannofossil zone: top of NP14a; planktonic foraminiferal zone: base of P10.
Age assignment: 48.6 Ma.
Discussion: lower Eocene sediments from the Norwegian–Greenland Sea, in particular in Hole 913B, are characterised by abundant glochidia and massulae of the hydropterid fern *Azolla*. *Azolla* spp. is also widespread in the early Eocene in the North Sea (Bujak and Mudge, 1994). In the Norwegian–Greenland Sea, the LO of *Azolla* spp. is coincident with the LO of *Eatonicysta ursulae*, which we directly correlate to Chron C21r.

FO *Cerebrocysta magna* (Cm)
Direct calibration: magnetic polarity chronozone: C21r.
Indirect calibration: calcareous nannofossil zone: top of NP14a; planktonic foraminiferal zone: base of P10.
Age assignment: 48.6 Ma.
Discussion: published range charts for the North Sea (Mudge and Bujak, 1996) indicate that the FO of *Cerebrocysta magna* occurs at the top of Bujak and Mudge's (1994) Subzone E2b, which they indirectly correlate to NP12. *Cerebrocysta magna* has not previously been recorded outside the North Sea, so temporal variation in its range is poorly known. We directly correlate the FO of *C. magna* to Chron C21r, which provides the first calibrated occurrence of this species outside the North Sea.

FO *Areosphaeridium ebdonii* (Ae)
Direct calibration: magnetic polarity chronozone: C21r–C21n transition.
Indirect calibration: calcareous nannofossil zone: top of NP14b; planktonic foraminiferal zone: P10.
Age assignment: 48.0 Ma.
Discussion: published range charts for the North Sea (Mudge and Bujak, 1996) indicate that the FO of *Areosphaeridium ebdonii* occurs in Zone E3c of Bujak and Mudge (1994), which is indirectly correlated to NP14a. *Areosphaeridium ebdonii* has not been previously recorded outside the North Sea, so our direct calibration to the GPTS constrains its total stratigraphic range.

LO *Hystrichostrogylon clausenii* (Hcl)
Direct calibration: magnetic polarity chronozone: C21n.
Indirect calibration: calcareous nannofossil zone: NP15a; planktonic foraminiferal zone: P10.
Age assignment: 47.1 Ma.
Discussion: the Lutetian interval in the Norwegian–Greenland Sea contains the LO of *Hystrichostrogylon clausenii*, which, according to its occurrence within the Glinde Formation of northwest Germany had been assigned to NP14 (Heilmann-Clausen and Costa, 1989). Bujak and Mudge (1994) used the LO of *H. clausenii* as a zonal marker and assigned the base of their E4c Subzone to NP15. However, their scheme has no direct calibration to the standard calcareous nannoplankton zonation, so they stated that it was possible that the lower part of E4c could correlate with the upper part of NP14. The palaeomagnetic constraint provided here indicates that the LO of *H. clausenii* occurs in Chron C21n, which corresponds to NP15a.

LO *Dracodinium pachydermum* (Dp)
Direct calibration: magnetic polarity chronozone: C21n.

Indirect calibration: calcareous nannofossil zone: NP15a; planktonic foraminiferal zone: P10.
Age assignment: 47.1 Ma.
Discussion: the LO of *Dracodinium pachydermum* is an important palynological event in the North Sea and has been assigned to NP14b (Bujak and Mudge, 1994). In our results from the Norwegian–Greenland Sea, the LO of *D. pachydermum* consistently occurs in Chron C21n and is assigned an age of 47.1 Ma, which corresponds to NP15a.

LO *Areoligera medusettiformis* plexus (Am)
Direct calibration: magnetic polarity chronozone: C21n.
Indirect calibration: calcareous nannofossil zone: NP15a; planktonic foraminiferal zone: P10.
Age assignment: 46.7 Ma.
Discussion: we include morphologically similar species *Areoligera medusettiformis*, *Areoligera senonensis* and *Areoligera coronata* in the *Areoligera medusettiformis* plexus. In the Norwegian–Greenland Sea, the *A. medusettiformis* plexus has its LO in Chron C21n, which is similar to other records from the Northern Hemisphere (Williams and Bujak, 1985).

LO *Hystrichosphaeropsis costae* (Hc)
Direct calibration: magnetic polarity chronozone: C21n.
Indirect calibration: calcareous nannofossil zone: NP15a; planktonic foraminiferal zone: P10.
Age assignment: 46.7 Ma.
Discussion: *Hystrichosphaeropsis costae* was formally described by Bujak (1994), with its LO being recorded from the North Sea *Cerebrocysta magna* Subzone (E4c), which was indirectly correlated to NP15 (Bujak and Mudge, 1994). *Hystrichosphaeropsis costae* is considered to be conspecific with *Hystrichosphaeropsis* sp. 1, which Heilmann-Clausen and Costa (1989) described from the Wusterheide research well, northwest Germany, where its LO is within the Glinde Formation, which is assigned to NP14. In the Norwegian–Greenland Sea, the LO of *H. costae* can be directly correlated to Chron C21n, and assigned an age of 46.7 Ma, which correlates to the lower part of NP15a.

LO *Adnatosphaeridium vittatum* (Av)
Direct calibration: magnetic polarity chronozone: C21n.
Indirect calibration: calcareous nannofossil zone: NP15a; planktonic foraminiferal zone: P10.
Age assignment: 46.6 Ma.
Discussion: in all three sites studied in the Norwegian–Greenland Sea, *Adnatosphaeridium vittatum* has a similar range to that recorded from the North Sea (Bujak, 1994; upper NP15). The LO of *A. vittatum* consistently occurs in Chron C21n, which is indirectly correlated to NP15a.

FO *Phthanoperidinium regalis-clithridium* complex (Pc)
Direct calibration: magnetic polarity chronozone: C20r.
Indirect calibration: calcareous nannofossil zone: NP15b; planktonic foraminiferal zone: upper P10.
Age assignment: 46.1 Ma.
Discussion: *Phthanoperidinium regalis* and *Phthanoperidinium clithridium* have a restricted range in the Lutetian in the North Sea (Bujak and Mudge, 1994; Bujak, 1994; Mudge and Bujak, 1996). These distinctive species were first described by Bujak (1994), and have not been previously recorded beyond the North Sea. The studied North Sea material consisted mainly of ditch cuttings and sampling was of too low a resolution to distinguish between the ranges of *P. regalis* and *P. clithridium* (Bujak, pers. commun. 2002). In the North Sea, the FOs of *P. regalis* and *P. clithridium* were indirectly correlated to NP15 (Mudge and Bujak, 1996).

Previous biostratigraphic studies of the Norwegian–Greenland Sea (Manum, 1976; Manum et al., 1989; Firth, 1996) were also of low sampling resolution and consequently the presence of *P. regalis* or *P. clithridium* were not recorded. *Phthanoperidinium clithridium* has been identified only in Hole 913B, with a range slightly higher than for *P. regalis*. For the purposes of this calibration, these two morphologically similar species have been grouped into a complex, and their combined ranges are used as datum events. In all three sites studied here, the FO of the *P. regalis-clithridium* complex occurs within Chron C20r.

LO *Cerebrocysta magna* (Cm)
Direct calibration: magnetic polarity chronozone: base of C20r.
Indirect calibration: calcareous nannofossil zone: base of NP15b; planktonic foraminiferal zone: P10.
Age assignment: 46.2 Ma.
Discussion: *Cerebrocysta magna* has a restricted stratigraphic range in the North Sea Basin, with its LO being recorded at the top of the Lutetian Subzone E4c of Bujak and Mudge (1994). In the Norwegian–Greenland Sea, the LO of *C. magna* consistently occurs at the base of Chron C20r.

LO *Lentinia wetzelii* (Lw)
Direct calibration: magnetic polarity chronozone: lower C20r.
Indirect calibration: calcareous nannofossil zone: base of NP15b; planktonic foraminiferal zone: base of P11.
Age assignment: 45.5 Ma.
Discussion: *Lentinia wetzelii* has been recorded from southern England, where it last appears at the top of Zone B-5 from the Bracklesham Beds of the Hampshire Basin, which are assigned to NP15 (Bujak, 1980; Williams and Bujak, 1985). In the Norwegian–Greenland Sea, the new palaeomagnetic reversal stratigraphy has constrained the LO of *L. wetzelii* to the lower part of Chron C20r, which corresponds to the base of NP15b.

LO *Diphyes ficusoides* (Df)
Direct calibration: magnetic polarity chronozone: C20r.
Indirect calibration: calcareous nannofossil zone: base of NP15b; planktonic foraminiferal zone: base of P11.
Age assignment: 45.4 Ma.
Discussion: in the North Sea, the LO of *D. ficusoides* has been assigned to NP15 (Bujak and Mudge, 1994). This age interpretation is based on the documented LO of *D. ficusoides* near the base of the Selsey Formation at Bracklesham Bay (Islam, 1983), which has been correlated with Bed X of Fisher (1862) at Whitecliff Bay, which Aubry (1985) assigned to NP15.

Diphyes ficusoides has also been documented in the Sables de Lede Formation in the Belgian Basin, which has also been assigned to NP15 (Verbeek, 1988; Verbeek et al., 1988; Bujak and Mudge, 1994). Our Norwegian–Greenland Sea palaeomagnetic reversal stratigraphy has constrained the LO of *D. ficusoides* to Chron C20r, with an age of 45.4 Ma, which corresponds to NP15b.

LO *Cerodinium depressum* (Cd)
Direct calibration: magnetic polarity chronozone: C20r.
Indirect calibration: calcareous nannofossil zone: NP15b; planktonic foraminiferal zone: P11.
Age assignment: 44.9 Ma.
Discussion: in the North Sea zonation of Bujak and Mudge (1994), *Cerodinium depressum* has its consistent LO in Subzone E4d, which is associated with NP15b. A numerical age for the LO of *C. depressum* in the North Sea has not been previously published. We assign an age of 44.9 Ma to the LO of *C. depressum* based on the direct calibration of this event with Chron C20r.

FO *Heteraulacacysta porosa* (Hp)
Direct calibration: magnetic polarity chronozone: C20r.
Indirect calibration: calcareous nannofossil zone: NP15b; planktonic foraminiferal zone: P11.
Age assignment: 44.8 Ma.
Discussion: the FO of *Heteraulacacysta porosa* has been recorded from NP16 in southern England (Bujak, 1980) and in the Labrador Sea (Head and Norris, 1989). Subsequent range charts from the North Sea (Mudge and Bujak, 1996) indicate that the FO of *Heteraulacacysta porosa* occurs in Bujak and Mudge's (1994) Subzone E4c, which was indirectly correlated to NP15a. Our results constrain the FO of *Heteraulacacysta porosa* to Chron C20r.

LO *Phthanoperidinium regalis-clithridium* complex (Pc)
Direct calibration: magnetic polarity chronozone: C20r.
Indirect calibration: calcareous nannofossil zone: NP15b; planktonic foraminiferal zone: P11.

Age assignment: 44.6 Ma.
Discussion: the LOs of *Phthanoperidinium regalis* and *Phthanoperidinium clithridium* were used by Bujak and Mudge (1994) as zonal markers in the middle Eocene (Lutetian) and were assigned to NP15 based solely on their correlation of the overlying and underlying subzones (Bujak and Mudge, 1994). In the Norwegian–Greenland Sea, the combined LOs of *P. regalis* and *P. clithridium* occur in Chron 20r, which corresponds to NP15b.

FO *Wetzeliella ovalis* (Wo)
Direct calibration: magnetic polarity chronozone: C20r.
Indirect calibration: calcareous nannofossil zone: NP15b; planktonic foraminiferal zone: P11.
Age assignment: 44.3 Ma.
Discussion: range charts for the North Sea (Mudge and Bujak, 1996) indicate that the FO of *Wetzeliella ovalis* occurs at the top of Bujak and Mudge's (1994) Subzone E6a, which indirectly correlates with NP15b. In the Norwegian–Greenland Sea, we directly correlate the FO of *Wetzeliella ovalis* to Chron C20r, which is associated with NP15b.

LO *Areosphaeridium ebdonii* (Ae)
Direct calibration: magnetic polarity chronozone: lower C20n.
Indirect calibration: calcareous nannofossil zone: NP15b–NP16; planktonic foraminiferal zone: base of P12.
Age assignment: 43.5 Ma.
Discussion: *Areosphaeridium ebdonii* has not been previously recorded outside the North Sea, where Bujak and Mudge (1994) used the LO of *A. ebdonii* to mark the top of their Subzone E5a, which was indirectly correlated to NP15. The location of this datum event varies between Chrons C20r and C20n in the studied Norwegian–Greenland Sea drill-holes (Figs. 5–7), so we assign the LO to Chron C20n.

LO super-abundant *Phthanoperidinium geminatum* (Pg)
Direct calibration: magnetic polarity chronozone: C20n.
Indirect calibration: calcareous nannofossil zone: NP16; planktonic foraminiferal zone: P12.
Age assignment: 42.9 Ma.
Discussion: at all three of the sites studied here, *P. geminatum* has two distinct abundance peaks, which provide additional datum events for correlation (cf. Firth, 1996). At Hole 913B, the earlier abundance event, as defined by the LO of super-abundant *P. geminatum*, is characterised by an almost mono-specific assemblage. Slight diachroneity exists in the LO of super-abundant *P. geminatum* within the Norwegian–Greenland Sea (Table 1). A slightly earlier LO of super-abundant *P. geminatum* occurs in the more basinal depositional environments that characterise holes 913B and 643A, in constrast to a slightly later LO at Hole 338, which is located on the outer slope of the Vøring Plateau. This may reflect varying palaeocirculation and ventilation regimes operating between slope and abyssal environments as a result of the tectonic evolution of the Norwegian–Greenland Sea during this period. In CSRS 3, the LO of super-abundant *P. geminatum* correlates with the upper part of Chron C20n (ca 42.9 Ma).

FO *Svalbardella cooksoniae* (Sc)
Direct calibration: magnetic polarity chronozone: C19r.
Indirect calibration: calcareous nannofossil zone: NP16; planktonic foraminiferal zone: P12.
Age assignment: 41.9 Ma.
Discussion: *Svalbardella cooksoniae* occurs in the upper Eocene in Spitsbergen (Manum, 1960; Manum and Throndsen, 1986) and in the Labrador Sea (Head and Norris, 1989). Manum (1976) recorded the FO of *Svalbardella cooksoniae* in sediments tentatively assigned to the middle Eocene. Our results confirm that in the Norwegian–Greenland Sea, the FO of *Svalbardella cooksoniae* occurs in middle Eocene sediments that are directly correlated to Chron C19r.

FO *Distatodinium ellipticum* (De)
Direct calibration: magnetic polarity chronozone: C19r.
Indirect calibration: calcareous nannofossil zone: NP16; planktonic foraminiferal zone: P12.

Age assignment: 41.7 Ma.
Discussion: In the North Atlantic, the FO of *Distatodinium ellipticum* has been directly correlated to NP16 (Damassa et al., 1990), which is consistent with our calibration from the Norwegian–Greenland Sea.

FO *Enneadocysta arcuata* (Ea)
Direct calibration: magnetic polarity chronozone: C19r.
Indirect calibration: calcareous nannofossil zone: NP16; planktonic foraminiferal zone: P12.
Age assignment: 41.7 Ma.
Discussion: the FO of *Enneadocysta arcuata* is recorded in southern England, where it first appears in Zone B-4, from the Bracklesham Beds of the Hampshire Basin, which are assigned to NP14 (Bujak, 1980; Williams and Bujak, 1985). However, in northwest Germany, the FO of *E. arcuata* has been recorded in middle Eocene strata assigned to NP16 (Köthe, 1990). In the Norwegian–Greenland Sea, we calibrate the FO of *E. arcuata* to Chron C19r, which correlates with NP16.

LO *Diphyes colligerum* (Dc)
Direct calibration: magnetic polarity chronozone: C19n.
Indirect calibration: calcareous nannofossil zone: NP16; planktonic foraminiferal zone: P12.
Age assignment: 41.3 Ma.
Discussion: the LO of *Diphyes colligerum* has been suggested by Williams (1975, 1977) and Williams et al. (1993) to indicate the E/O boundary, based on material from offshore eastern Canada and on a literature review of worldwide occurrences. However, Brinkhuis and Biffi (1993) demonstrated that *D. colligerum* persists into the lower Oligocene in Italy. The last common occurrence (LCO) of *D. colligerum* has been used as a middle Eocene zonal marker in the North Sea (Bujak and Mudge, 1994), and is assigned to NP16, although rare specimens have been documented to extend to the top of the Priabonian. *Diphyes colligerum* is considered to be a temperature-sensitive species that migrated southward at the onset of cooler water conditions (Brinkhuis and Biffi, 1993; Bujak and Mudge, 1994). This would explain its progressively southward migrating last appearances in the Norwegian–Greenland Sea, its LCO in the North Sea in the Bartonian, and its persistence into the lower Rupelian in Italy. Sporadic occurrences of *D. colligerum* in North Sea Priabonian strata may have resulted from periodic migration into the basin during relatively brief warmer periods (Bujak and Mudge, 1994). Despite *D. colligerum* being a thermophilic taxon with a diachronous range, the LO of this species consistently occurs in Chron C19n within the Norwegian–Greenland Sea.

LO abundant *Phthanoperidinium geminatum* (Pg)
Direct calibration: magnetic polarity chronozone: C19n.
Indirect calibration: calcareous nannofossil zone: NP16; planktonic foraminiferal zone: P12.
Age assignment: 41.3 Ma.
Discussion: *Phthanoperidinium geminatum* has its worldwide LO at the top of the middle Eocene (Williams and Bujak, 1985; top of NP17). As mentioned above, *P. geminatum* has two distinct abundance peaks in the Norwegian–Greenland Sea. The later acme event occurred in Chron C19n (ca. 41.3 Ma) and is defined by the LO of abundant *P. geminatum*. The LO of abundant *P. geminatum* also coincides with the LO of *Diphyes colligerum*.

LO *Areoligera tauloma* (At)
Indirect calibration: magnetic polarity chronozone: C18r; calcareous nannofossil zone: NP16-NP17 boundary; planktonic foraminiferal zone: P13.
Age assignment: 40.2 Ma.
Discussion: Bujak and Mudge (1994) defined the top of their North Sea E7a Subzone according to the LO of *Areoligera tauloma*. Their definition was based on re-examination of material from the Hampshire Basin, which indicated that *A. tauloma* last appears at the top of Zone BAR-1 just below the NP16–NP17 boundary in the Barton Beds. In the CSRS 3 from the Norwegian–Greenland Sea, the LO of *A. tauloma*, based on its occurrence in holes 643A and 338, corresponds with Chron C18r, which suggests that this datum occurs at a similar stratigraphic level as in the North

Sea (Fig. 12). However, the only direct correlation of this datum event to the GPTS in the Norwegian–Greenland Sea is in Hole 643A, where it correlates to Chron C19n–C19r, whereas in Hole 338, the LO of *A. tauloma* occurs in an interval of uncertain polarity that we indirectly correlate to Chron C18n.2n (Figs. 6 and 7; Table 1). Therefore, we can only provide an *indirect* calibration of this event with Chron C18r.

LO *Wetzeliella ovalis* (Wo)
Indirect calibration: magnetic polarity chronozone: C18r; calcareous nannofossil zone: NP16-NP17 boundary; planktonic foraminiferal zone: P13.
Age assignment: 40.2 Ma.
Discussion: in the North Sea, the LO of *Wetzeliella ovalis* occurs at the top of Subzone E6c (Bujak and Mudge, 1994), which correlates with NP16. The stratigraphic location of this datum event varies among the studied Norwegian–Greenland Sea drill-holes (Figs. 5–7; Table 1). In holes 913B and 643A the LO of *W. ovalis* is directly correlated to Chrons C20r and C19n, respectively, whereas, in Hole 338, it occurs in an interval of uncertain polarity, which we indirectly correlate to Chron C18n.2n. A slightly earlier LO of *W. ovalis* occurs in the more basinal depositional environments that characterise holes 913B and 643A, in contrast to a slightly later LO at Hole 338, which may reflect the continued influence of a brackish water environment on the outer Vøring Plateau. Therefore, we can only provide an *indirect* calibration of this event with Chron C18r (40.2 Ma).

FO *Rhombodinium rhomboideum* (Rr)
Direct calibration: magnetic polarity chronozone: C18n.2n.
Indirect calibration: calcareous nannofossil zone: base of NP17; planktonic foraminiferal zone: P13–P14 boundary.
Age assignment: 39.9 Ma.
Discussion: range charts for the North Sea (Mudge and Bujak, 1996) indicate that the FO of *Rhombodinium rhomboideum* occurs at the top of Bujak and Mudge's (1994) Subzone E6a, which correlates to NP15b. We calibrate the FO of *R. rhomboideum* to Chron C18n.2n, which correlates with the base of NP17, which suggests that this datum occurs stratigraphically higher in the Norwegian–Greenland Sea than in the North Sea.

LO *Rhombodinium rhomboideum* (Rr)
Direct calibration: magnetic polarity chronozone: C18n.1r.
Indirect calibration: calcareous nannofossil zone: NP17; planktonic foraminiferal zone: P14.
Age assignment: 39.6 Ma.
Discussion: in the North Sea, the LO of *Rhombodinium rhomboideum* occurs at the top of Subzone E6c, which was correlated to the upper part of NP16 (Bujak and Mudge, 1994). *Rhombodinium rhomboideum* has also has been recorded from the southern Netherlands (De Coninck, 1986), with its LO occurring in sediments tentatively assigned to NP16 by Verbeek (1988). We calibrate the LO of *R. rhomboideum* to Chron C18n.1r, which is associated with the lower part of NP17.

LO *Rottnestia borussica* (Rb)
Direct calibration: magnetic polarity chronozone: C18n.1r.
Indirect calibration: calcareous nannofossil zone: NP17; planktonic foraminiferal zone: P14.
Age assignment: 39.6 Ma.
Discussion: *Rottnestia borussica* last appears in the Hampshire Basin (Bujak, 1979, 1980) in strata assigned to NP17 by Aubry (1983, 1985). In the North Sea zonation of Bujak and Mudge (1994), the LO of *R. borussica* was assigned to NP17 based on indirect correlation with the Hampshire Basin. However, Brinkhuis and Biffi (1993) demonstrated that *R. borussica* persists into the Oligocene in Italy. In the Norwegian–Greenland Sea, the LO of *R. borussica* is constrained to Chron C18n.1r, which corresponds to NP17, and which suggests that this datum occurs at a similar stratigraphic level as in the North Atlantic and North Sea.

FO *Areoligera*? *semicirculata* (As)
Direct calibration: magnetic polarity chronozone: C18n.1n.
Indirect calibration: calcareous nannofossil zone: NP17; planktonic foraminiferal zone: P14.

Age assignment: 38.5 Ma.
Discussion: in previous studies from the Norwegian–Greenland Sea, *Areoligera*? *semicirculata* was recorded from Hole 643A, in the upper Eocene to Oligocene (Williams and Manum, 1999; Manum et al., 1989, as *Glaphyrocysta intricata*). The FO of *A.*? *semicirculata* has been used to mark the lower Oligocene in Belgium (Stover and Hardenbol, 1994) and in central Italy where it has been directly correlated to the base of Chron C13n (Brinkhuis and Biffi, 1993). In the Norwegian–Greenland Sea, we calibrate the FO of *A.*? *semicirculata* to the upper Eocene (C18n.1n).

LO *Phthanoperidinium distinctum* (Pd)
Direct calibration: magnetic polarity chronozone: C17n.2n.
Indirect calibration: calcareous nannofossil zone: NP17; planktonic foraminiferal zone: P15.
Age assignment: 37.7 Ma.
Discussion: *Phthanoperidinium distinctum* was described by Bujak (1994) and has only been previously recorded outside the North Sea Basin by Firth (1996). Its LO was used by Bujak and Mudge (1994) as a zonal marker for the middle Eocene (North Sea Subzone E6b; NP16). The consistent and common occurrence of *P. distinctum* up to Chron C17n.2n at all three sites studied from the Norwegian–Greenland Sea suggests that it is unlikely to be reworked, and, therefore, that its range extends above that reported in the North Sea by Bujak and Mudge (1994; see also Firth, 1996).

LO *Heteraulacacysta porosa* (Hp)
Direct calibration: magnetic polarity chronozone: C16r.
Indirect calibration: calcareous nannofossil zone: NP18; planktonic foraminiferal zone: P15.
Age assignment: 36.4 Ma.
Discussion: *Heteraulacacysta porosa* is reported by Bujak (1980) and Powell (1992) as having a narrow stratigraphic range within the Bartonian (upper middle Eocene). *Heteraulacacysta porosa* has been used as a middle Eocene zonal marker in the North Sea (Bujak and Mudge, 1994), based on its LO from the Barton Beds of the Hampshire Basin (Bujak, 1980) in strata assigned to NP17 (Aubry, 1983, 1985). In the North Sea, the LO of *H. porosa* occurs at the Bartonian–Priabonian boundary (37 Ma; Bujak and Mudge, 1994), whereas in the Norwegian–Greenland Sea it ranges slightly higher into the Priabonian (Chron C16r; ~36.4 Ma; Fig. 12).

LO *Areosphaeridium michoudii* (Ami)
Direct calibration: magnetic polarity chronozone: C16n.1n.
Indirect calibration: calcareous nannofossil zone: NP19–NP20; planktonic foraminiferal zone: P16.
Age assignment: 35.4 Ma.
Discussion: published records of *Areosphaeridium michoudii* are confined to the North Sea (Bujak and Mudge, 1994; Gradstein et al., 1992) and the Norwegian–Greenland Sea (Firth, 1996), where this species is reported to have its LO slightly lower in the upper Eocene than *Areosphaeridium diktyoplokum*. In the North Sea zonation of Bujak and Mudge (1994), the top of the *Areosphaeridium michoudii* Subzone, as defined by the LO of *A. michoudii*, was indirectly correlated to NP18, due to its stratigraphic position below their *Areosphaeridium diktyoplokum* Subzone (E8b) and above their *Heteraulacacysta porosa* Biozone (E7). We directly calibrate the LO of *A. michoudii* to Chron C16n.1n, which suggests a similar range to that recorded in the North Sea (Gradstein et al., 1992; Bujak and Mudge, 1994; see Fig. 12). The upper range of this species is sometimes truncated by an upper Eocene–Oligocene hiatus, which appears to be the case for holes 338 and 643A.

LO *Svalbardella cooksoniae* (Sc)
Direct calibration: magnetic polarity chronozone: C15r–C13r.
Indirect calibration: calcareous nannofossil zone: NP19–NP21; planktonic foraminiferal zone: P16–P18.
Age assignment: 35.1–33.6 Ma.
Discussion: *Svalbardella cooksoniae* has a reported LO in the early Oligocene from northwestern Europe (Costa et al., 1988). *Svalbardella cooksoniae* has also been recorded from lower Oligocene strata in the Labrador Sea, where its LO is correlated

to NP22 (Head and Norris, 1989). In the Norwegian–Greenland Sea, a comparison between Hole 985A and Hole 643A by Williams and Manum (1999) using numerical ages from Goll (1989, unpubl. data) suggests that the LO of *S. cooksoniae* occurs at 31.9 Ma. The only previously recorded LO of *S. cooksoniae* with magnetostratigraphic control is from Italy, where it has been directly calibrated to Chron C12r (Brinkhuis and Biffi, 1993; Brinkhuis, 1994). In CSRS 3, the LO of *S. cooksoniae* correlates with Chron C13r (ca 33.6 Ma). However, in Hole 913B, the LO of

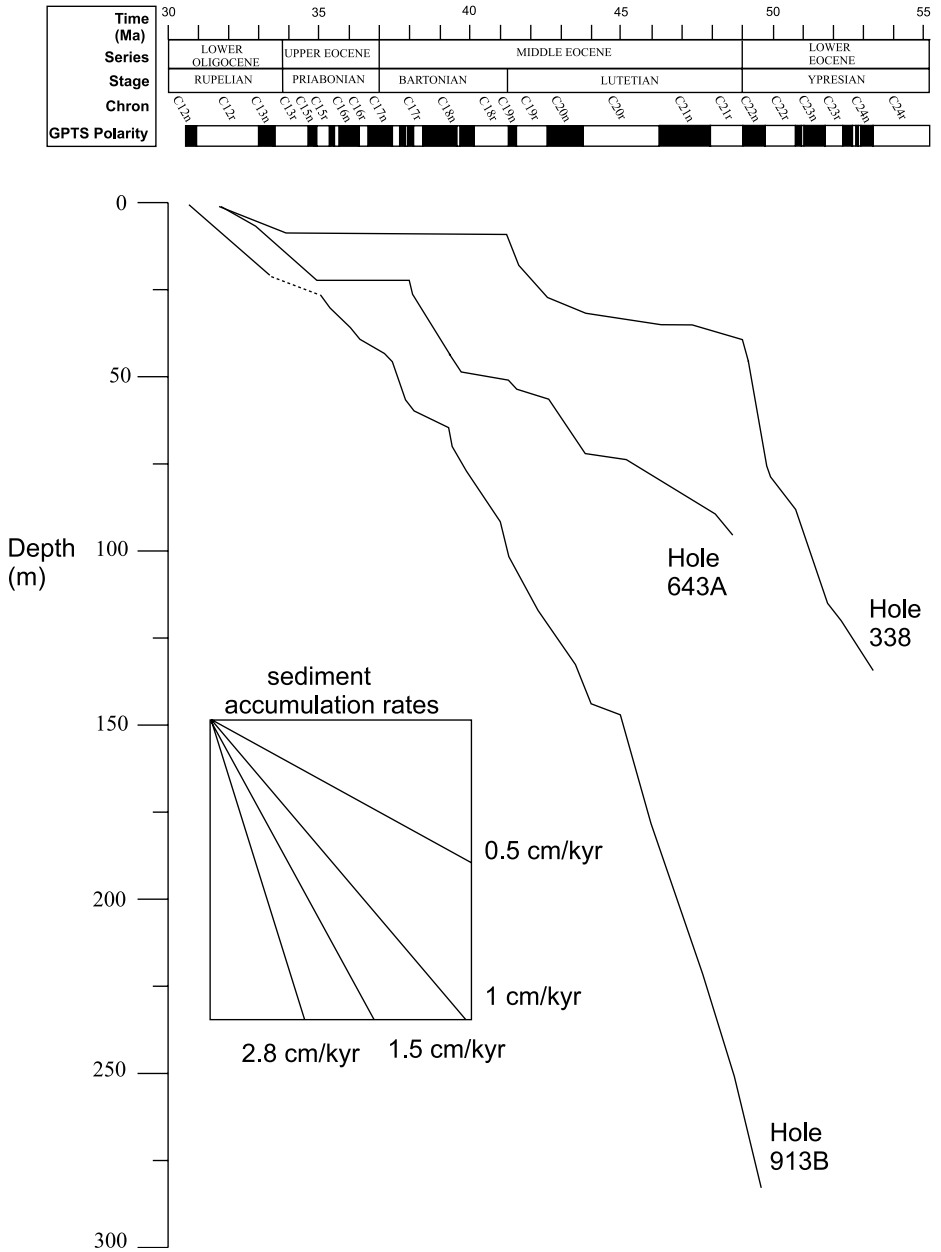

Fig. 13. Stratigraphical nomograph showing age-depth curves for holes 913B, 338 and 643A. The timescale of Cande and Kent (1992, 1995) and Berggren et al. (1995) is used. The age–depth lines indicate average rates of sediment accumulation.

S. cooksoniae is directly correlated with C15r (Fig. 5). We therefore calibrate this datum event to an interval between Chrons C15r and C13r.

LO *Melitasphaeridium pseudorecurvatum* (Mp)

Direct calibration: magnetic polarity chronozone: base of C15n.

Indirect calibration: calcareous nannofossil zone: NP19–NP20; planktonic foraminiferal zone: P16.

Age assignment: 34.7 Ma.

Discussion: *Melitasphaeridium pseudorecurvatum* has been reported to have a worldwide LO in the upper Eocene, and was indirectly correlated to the base of NP19 (Williams and Bujak, 1985). Brinkhuis and Biffi (1993) recorded the LO of *M. pseudorecurvatum* from the upper Eocene of central Italy, with a direct palaeomagnetic correlation to Chron C15n. In holes 913B and 643A from the Norwegian–Greenland Sea, the LO of *M. pseudorecurvatum* is directly correlated to Chrons C15r–C15n, whereas, in Hole 338, it occurs in the interval of uncertain polarity that we indirectly correlate to Chron C13r (Figs. 5–7; Table 1). It is therefore preferable to calibrate this datum event to Chron C15n based on the more robust magnetostratigraphic constraint provided for holes 913B and 643A.

LO *Areosphaeridium diktyoplokum* (Ad)

Direct calibration: magnetic polarity chronozone: C13n–C13r

Indirect calibration: calcareous nannofossil zone: NP21; planktonic foraminiferal zone: P17–P18 boundary.

Age assignment: 33.6–33.4 Ma

Discussion: Berggren et al. (1995, pp. 197–198) stated that the 'position and age of the E/O boundary are intimately associated with problems pertaining to the litho- and biostratigraphic characteristics and limits of the upper Eocene Priabonian and lower Oligocene 'standard' stages'. Central to this problem is the LO of *A. diktyoplokum*, which Brinkhuis and Biffi (1993) indicated was consistently in lower Oligocene strata in Italy, and is therefore not associated with the E/O boundary as currently defined by the LO of hantkeninid foraminifera at Massignano. Subsequently, Brinkhuis and Visscher (1995), based on the above results, recommended that the upper boundary of the Priabonian at Priabona be retained, so that the E/O boundary would be coincident with the LO of *A. diktyoplokum* in Chron C13n at Priabona, rather than with the LO of hantkeninids at Massignano (C13r). However, the issue is still unresolved, so the current boundary definition and Global Standard Stratotype Section and Point at Massignano, based on the timescale of Berggren et al. (1995) and Cande and Kent (1995) is used here.

Williams et al. (1993) and Stover and Williams (1995) reviewed the published records of *A. diktyoplokum* and concluded that its LO is at the top of the Eocene. Many authors who associate the LO of *A. diktyoplokum* with the E/O boundary have suggested that Oligocene occurrences of *A. diktyoplokum* are due to reworking (Williams and Bujak, 1985; Costa et al., 1988; Stover et al., 1988; Head and Norris, 1989). Hole 913B yielded the only material from this study that has sporadic Oligocene occurrences of *A. diktyoplokum*. These sporadic occurrences are thought to be reworked due to their association with a reworking interval

Plate I. The species name is followed by the ODP/DSDP site number; sample depth (mbsf) in which the specimen was found and the England Finder references for the specimen on the slide. All scale bars = 25 μm.

1. *Areoligera medusettiformis*; 338; 318.15 mbsf; X22-4.
2. *Areoligera tauloma*; 338; 462.00 mbsf; G38-1.
3. *Areosphaeridium diktyloplokum*; 338; 268.41 mbsf; X21-0.
4. *Areosphaeridium ebdonii*; 913B; 594.08 mbsf; F38-2.
5. *Areosphaeridium michoudii*; 913B; 499.34 mbsf; N42-4.
6. *Cerebrocysta magna*; 913B; 618.54 mbsf; R18-2.
7. *Cerodinium depressum*; 913B; 592.57 mbsf; Q16-0.
8. *Charlesdowniea columna*; 913B; 709.66 mbsf; P17-3.
9. *Chiropteridium galea*; 913B; 425.88 mbsf; M17-1.

Plate I

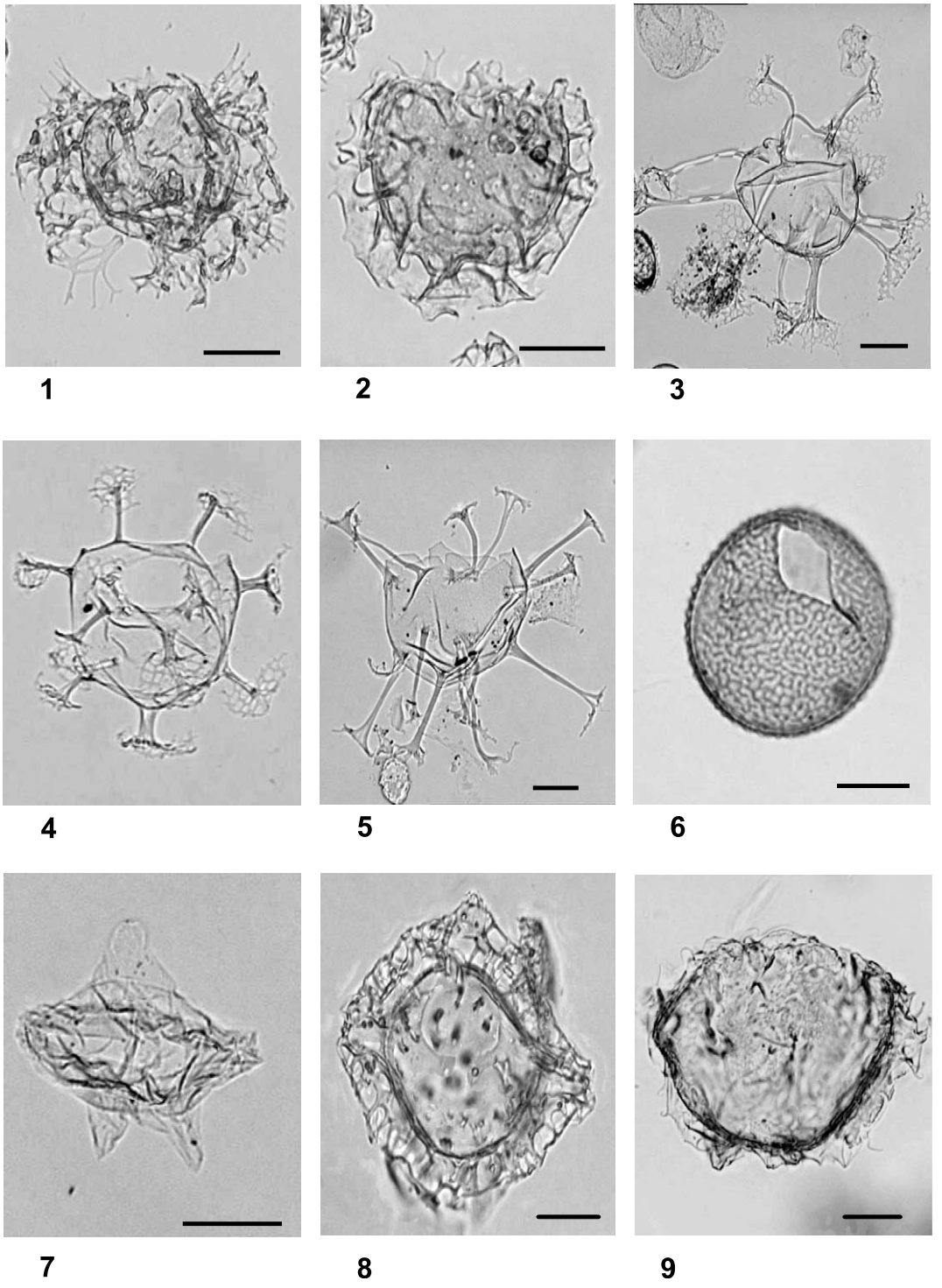

as identified by large numbers of Cretaceous palynomorphs (Firth, 1996). However, from all three cores studied here, *A. diktyoplokum* is consistently present at stratigraphically lower levels, and its LO is in sediments that are correlated to Chron C13n–C13r. The LO of *A. diktyoplokum* in the Norwegian–Greenland Sea is equivalent to the top of the *A. diktyoplokum* Biozone (E8) of the North Sea (Bujak and Mudge, 1994) and Zone T5 of Gradstein et al. (1992), which these authors take to mark the top of the Eocene (see Fig. 12).

FO *Chiropteridium galea* (Cg)
Direct calibration: magnetic polarity chronozone: C13n–C13r.
Indirect calibration: calcareous nannofossil zone: NP21–NP22 boundary; planktonic foraminiferal zone: P18.
Age assignment: 33.6–33.2 Ma.
Discussion: the FO of *Chiropteridium galea* has been used to mark the upper Eocene (Williams and Bujak, 1985, as *C. dispersum*; and Damassa et al., 1990, as *C. mespilanum*) and lower Oligocene (Bujak, 1980, as *C. dispersum*; and Head and Norris, 1989, as *C. mespilanum*). In the Norwegian–Greenland Sea, the FO of *C. galea* occurs in the lower Oligocene, and correlates to an interval around Chron C13n–C13r.

FO *Chiropteridium lobospinosum* (Cl)
Direct calibration: magnetic polarity chronozone: C13n–C13r.
Indirect calibration: calcareous nannofossil zone: NP21–NP22 boundary; planktonic foraminiferal zone: P18.
Age assignment: 33.6–33.2 Ma.
Discussion: *Chiropteridium lobospinosum* is not considered to range below the Oligocene (Williams and Bujak, 1985; Williams et al., 1993; Firth, 1996). Powell (1992) correlated the FO of *C. lobospinosum* with the middle part of NP23. We directly calibrate the FO of *C. lobospinosum* to an interval around Chron C13n–C13r.

FO *Spiniferites* sp. 1 sensu Manum et al., 1989 (Ssp1)
Direct calibration: magnetic polarity chronozone: C13n–C13r.
Indirect calibration: calcareous nannofossil zone: NP21–NP22 boundary; planktonic foraminiferal zone: P18.
Age assignment: 33.6–33.2 Ma.
Discussion: *Spiniferites* sp. 1 sensu Manum et al., 1989 has a restricted stratigraphic range in the early Oligocene of the Outer Vøring Plateau. This species has also been identified from the lower Oligocene at Hole 985A (ODP Leg 162), where it was informally described (Williams and Manum, 1999). A comparison between Hole 985A and Hole 643A using numerical ages from Goll (1989, unpubl. data) suggests that the FO of *Spiniferites* sp. 1 sensu Manum et al., 1989 occurred at 31.6 Ma (Williams and Manum, 1999). We calibrate the FO of *Spiniferites* sp. 1 sensu Manum et al., 1989 to an interval around Chron C13n–C13r (33.6–33.2 Ma).

FO *Wetzeliella gochtii* (Wg)
Direct calibration: magnetic polarity chronozone: C13n–C13r.

Plate II. The species name is followed by the ODP/DSDP site number; sample depth (mbsf) in which the specimen was found and the England Finder references for the specimen on the slide. All scale bars = 25 μm.

1. *Diphyes colligerum*; 338; 287.35 mbsf; R22-0.
2. *Diphyes ficusoides*; 913B; 560.68 mbsf; O38-1.
3. *Dracodinium pachydermum*; 913B; 646.12 mbsf; O13-0.
4. *Eatonicysta ursulae*; 913B; 705.23 mbsf; M24-2.
5. *Heteraulacacysta porosa*; 913B; 516.89 mbsf; N40-4.
6. *Hystrichosphaeropsis costae*; 913B; 661.54 mbsf; R20-3.
7. *Hystrichostrogylon clausenii*; 338; 289.75 mbsf; F26-1.
8. *Lentinia wetzelii*; 913B; 589.57 mbsf; R44-3.
9. *Melitasphaeridium pseudorecurvatum*; 913B; 468.54 mbsf; Q34-4.

Plate II

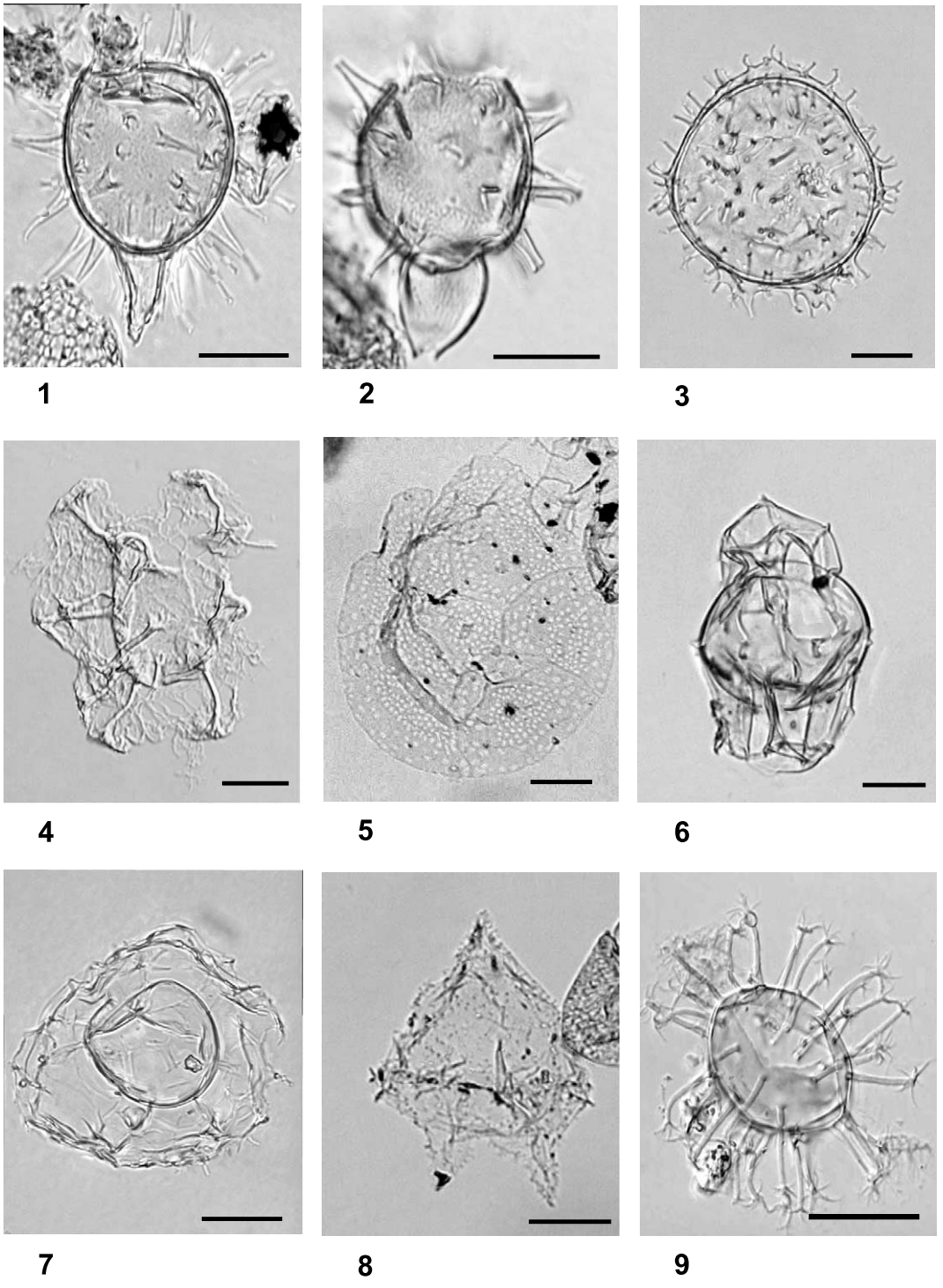

Indirect calibration: calcareous nannofossil zone: NP21–NP22 boundary; planktonic foraminiferal zone: P18.
Age assignment: 33.6–33.2 Ma.
Discussion: the FO of *Wetzeliella gochtii* is commonly used to recognise the lower Oligocene (Williams and Bujak, 1985). *Wetzeliella gochtii* has been recorded in the early Oligocene from northwestern Europe, with direct calibration to the base of NP22 (Costa and Downie, 1976; Williams and Bujak, 1985; Powell, 1992), although a subsequent zonation by Costa et al. (1988) correlated the FO of *W. gochtii* with NP21. In central Italy, Brinkhuis and Biffi (1993) recorded the FO of *W. gochtii* in their *Reticulatosphaeridium actinocoronata* Interval Zone, which directly correlates with the middle of NP21. Its FO in the Norwegian–Greenland Sea is directly calibrated to an interval around Chron C13n–C13r, which indirectly correlates with an interval around the NP21–NP22 boundary.

LO *Spiniferites* sp. 1 sensu Manum et al., 1989 (Ssp1)
Direct calibration: magnetic polarity chronozone: C12r.
Indirect calibration: calcareous nannofossil zone: NP23; planktonic foraminiferal zone: P18.
Age assignment: 31.0 Ma.
Discussion: a comparison between Hole 985A and Hole 643A using numerical ages from Goll (1989, unpubl. data) suggests that the LO of *Spiniferites* sp. 1 sensu Manum et al., 1989 occurs at 31.3 Ma (Williams and Manum, 1999). Development of a palaeomagnetic reversal stratigraphy for holes 643A and 913B in this study suggests that *Spiniferites* sp. 1 sensu Manum et al., 1989 has its LO in the upper part of Chron 12r (~30.9 Ma).

6. Discussion

6.1. Stratigraphic record of the Norwegian–Greenland Sea

Correlation of the stratigraphic record preserved in holes 913B, 338 and 643A with the GPTS (Fig. 13), enables comparison of sediment accumulation rates for the three holes. The sediment accumulation rate at Hole 338 decreased from 2.8 cm/kyr in the Ypresian to <0.5 cm/kyr in the Lutetian. This reduction in sediment accumulation rate coincided with a lithological transition from terrigeneous muds to pelagic oozes, which indicates a change in sediment source. Sedimentation rates at Hole 913B and 643A were comparatively stable at 1.5–2.8 cm/kyr, and 0.5 cm/kyr, respectively.

A stratigraphic hiatus has been identified in Hole 338, which spans an 8-m.y. period from the base of the Bartonian in the middle Eocene to the base of the Rupelian in the lower Oligocene. The hiatus at Hole 338 partially overlaps with a 3.5-m.y. hiatus at Hole 643A, which suggests an underlying regional cause. The distribution of hiatuses has been associated with glacioeustatic lowering of sea level and intensification of deep-water circulation due to high latitude cooling during the late Eocene (Kennett, 1977; Keller et al., 1987; Miller et al., 1987; Miller, 1992;

Plate III. The species name is followed by the ODP/DSDP site number; sample depth (mbsf) in which the specimen was found and the England Finder references for the specimen on the slide. All scale bars = 25 μm.

1. *Rhombodinium rhomboideum*; 913B; 500.65 mbsf; H25-3.
2. *Phthanoperidinium geminatum*; 913B; 541.34 mbsf; P26-0.
3. *Phthanoperidinium distinctum*; 913B; 521.97 mbsf; V19-1.
4. *Phthanoperidinium clithridium*; 913B; 582.94 mbsf; O45-3.
5. *Phthanoperidinium regalis*; 913B; 589.57 mbsf; G35-0.
6. *Rottnestia borussica*; 913B; 502.15 mbsf; O25-1.
7. *Spiniferites* sp. 1 sensu Manum et al., 1989; 643A; 463.20 mbsf; V38-3.
8. *Svalbardella cooksoniae*; 913B; 513.84 mbsf; Y37-2.
9. *Wetzeliella gochtii*; 913B; 444.70 mbsf; O31

Plate III

1

2

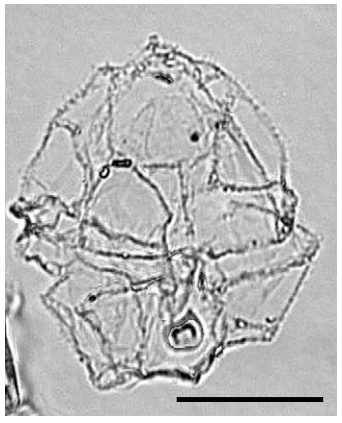

3

4

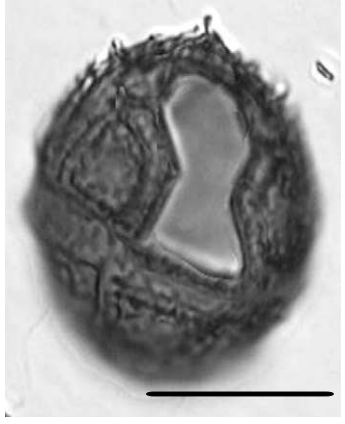

5

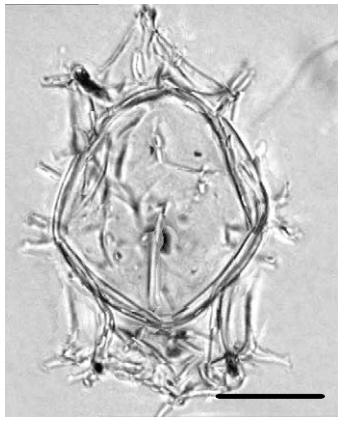

6

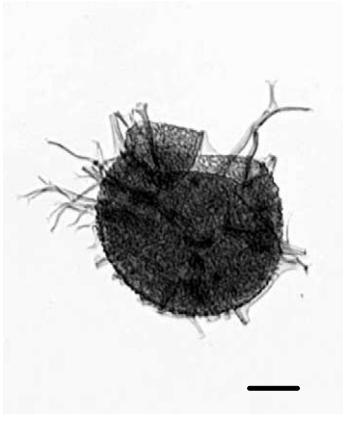

7

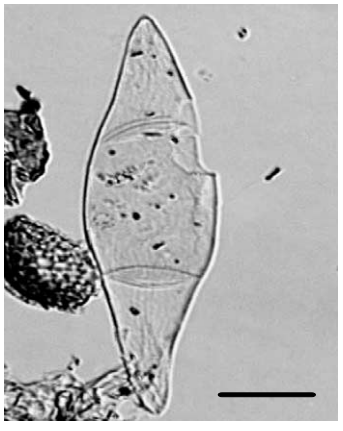

8

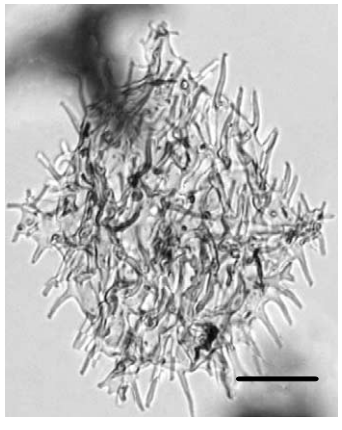

9

Abreu and Anderson, 1998; Zachos et al., 2001). These unconformities coincide with major seismic reflectors (A′ and ME, respectively; Goll, 1989) at holes 338 and 643A (Talwani et al., 1976; Skogseid and Eldholm, 1989). A coeval unconformity occurs in the North Sea Alba sequence, as indicated by a significant upper Eocene seismic reflector (Neal et al., 1994).

No stratigraphic hiatuses have been identified at Hole 913B, where a relatively complete Eocene sequence was recovered. This partly reflects the location of Hole 913B in the deep Greenland Basin, where it was likely to have been sheltered from current activity that might have been responsible for truncating sedimentary sequences in adjacent shallow water settings during the late Eocene. Hole 913B therefore contains the most complete and best-preserved record of the Eocene to Oligocene interval in the Northern Hemisphere high latitudes.

The dinocyst assemblages documented here also show affinities with the North Atlantic, as indicated by coeval assemblages from offshore eastern Canada (Williams, 1975), and also with those from southern England (Bujak, 1980). However, direct comparison with these zonations has proved problematical, because directly calibrated ages are not available for the main datum events in the latter two studies. Direct calibration to the GPTS, as achieved in the present study, marks a significant step forward in providing precise age calibration of Eocene and Oligocene dinocyst assemblages in the Norwegian–Greenland Sea.

7. Conclusions

Extensive calcite dissolution has limited the biostratigraphic usefulness of calcareous microfossils in Eocene–Oligocene sediments from the Norwegian–Greenland Sea. Our results indicate that dinocyst biostratigraphy in high-latitude sediments of this age is not only a viable alternative to calcareous microfossil biostratigraphy, but that it can be an important primary biostratigraphic tool.

In addition to previous dinocyst biostratigraphic studies from the Norwegian–Greenland Sea, we have identified many age-diagnostic species that have enabled the development of the first detailed Eocene–Oligocene dinocyst stratigraphy for this region. In addition, successful development of a robust magnetic polarity stratigraphy for holes 913B, 338 and 643A has provided independent age control and has enabled the calibration of a composite standard reference section to the GPTS. The dinocyst assemblages recovered in this study have affinities with those from the North Sea and North Atlantic, which enables regional correlation.

An upper Eocene hiatus at holes 338 and 643A is apparently coeval with those from the North Sea, which suggests a regional cause such as intensification of deep-water circulation and/or glacioeustatic lowering of sea level. In contrast, Hole 913B from the deep Greenland Basin has an almost complete Eocene to Oligocene stratigraphic sequence, which provides the only detailed record from the Norwegian–Greenland Sea of this phase of Earth history. The dinocyst datum events identified here from the Norwegian–Greenland Sea provide a magnetostratigraphically calibrated framework for future studies from Northern Hemisphere high-latitude sediments.

Acknowledgements

We are indebted to Prof. S. Manum for help at the University of Oslo with reviewing slides from Hole 643A. We also thank Dr. G.L. Williams and Dr. H. Brinkhuis for taxonomic advice, Dr. J.P. Bujak for help with identifying specific North Sea dinocysts and for providing valuable information on their ranges, and S. Akbari for help during palynological processing. Our thanks are also extended to Dr. Martin Head (Cambridge University) and one anonymous reviewer for their helpful suggestions, which have greatly improved the final manuscript. We also thank the American Association of Stratigraphic Palynologists (AASP), The Geological Society of London, The Micropalaeontological Society and the Natural Environment Research Council for funding this work.

Taxonomic appendix

Full author citations for the dinocyst taxa discussed are given by Williams et al. (1998). Plates refer to Plates I–III.

Species	*Plate*	*Fig.*
Adnatosphaeridium vittatum Williams and Downie, 1966	–	
Areoligera coronata (O. Wetzel, 1933) Lejeune-Carpentier, 1938	–	
Areoligera medusettiformis (O. Wetzel, 1933), Lejeune-Carpentier 1938 sensu Eaton, 1976	I	1
Areoligera semicirculata (Morgenroth, 1966b), Stover and Evitt, 1978	–	
Areoligera senonensis Lejeune-Carpentier, 1938	–	
Areoligera tauloma Eaton, 1976	I	2
Areosphaeridium diktyoplokum Klump, 1953	I	3
Areosphaeridium ebdonii Bujak, 1994	I	4
Areosphaeridium michoudii Bujak, 1994	I	5
Batiacasphaera compta Drugg, 1970	–	
Cerebrocysta magna Bujak, 1994	I	6
Cereodinium depressum (Morgenroth, 1966a), Lentin and Williams, 1987	I	7
Charlesdowniea coleothrypta Williams and Downie 1966	–	
Charlesdowniea columna (Michoux, 1988), Lentin and Williams, 1993	I	8
Chiropteridium galea (Maier, 1959) Sarjeant, 1983	I	9
Chiropteridium lobospinosum (Gocht in Weiler, 1956) Gocht, 1960	–	
Cordosphaeridium funiculatum Morgenroth, 1966a	–	
Diphyes colligerum (Deflandre and Cookson, 1955) Cookson, 1965	II	1
Diphyes ficusoides Islam, 1983	II	2
Distatodinium ellipticum (Cookson, 1965) Eaton, 1976	–	
Dracodinium pachydermum Caro, 1973) Costa and Downie, 1979	II	3
Eatonicysta ursulae (Morgenroth, 1966), Stover and Evitt, 1978	II	4
Enneadocysta arcuata (Eaton, 1971) Stover and Williams, 1995	–	
Glaphyrocysta intricata (Eaton, 1971) Stover and Evitt, 1978	–	
Heteraulacacysta porosa Bujak, 1980	II	5
Hystrichosphaeropsis costae Bujak, 1994	II	6
Hystrichostrogylon clausenii Bujak, 1994	II	7
Hystrichosphaeridium tubiferum (Ehrenberg, 1838) Deflandre, 1937	–	
Lentinia wetzelii (Morgenroth, 1966a) Bujak in Bujak et al., 1980	II	8
Melitasphaeridium pseudorecurvatum (Morgenroth, 1966a) Bujak et al., 1980	II	9
Phthanoperidinium clithridium Bujak, 1994	III	4
Phthanoperidinium distinctum Bujak, 1994	III	3
Phthanoperidinium geminatum Bujak in Bujak et al., 1980	III	2
Phthanoperdinium powellii Bujak, 1994	–	
Phthanoperidinium regalis Bujak, 1994	III	5
Reticulatosphaera actinocoronata (Benedek, 1972) Bujak and Matsuoka, 1986	–	
Rhombodinium rhomboideum (Alberti, 1961) Lentin and Williams, 1973	III	1
Rottnestia borussica (Eisenack, 1954), Cookson and Eisenack, 1961	III	6
Spiniferites sp. 1 of Manum et al., 1989	III	7
Svalbardella cooksoniae Manum, 1960	III	8
Wetzeliella gochtii Costa and Downie, 1976	III	9
Wetzeiella ovalis Eisenack, 1954	–	

References

Abreu, V.S., Anderson, J.B., 1998. Glacial eustasy during the Cenozoic: Sequence stratigraphic implications. AAPG Bull. 82, 1385–1400.

Acton, G.D., Okada, M., Clement, B.M., Lund, S.P., Williams, T., 2002. Paleomagnetic overprints in ocean sediment cores and their relationship to shear deformation caused by piston coring. J. Geophys. Res. 107, doi:10.1029/2001JB000518.

Armstrong, H.A., 1999. Quantitative biostratigraphy. In: Harper, D.A.T. (Ed.), Numerical Palaeobiology. Wiley, Chichester, pp. 181–226.

Aubry, M., 1983. Biostratigraphie du Paléogene épicontinental de l' Europe du Nord-Ouest, étude fondéé sur les nannofossils calcaires. Doc. Lab. Géol. Lyon 89.

Aubry, M.P., 1985. Northwestern European Paleogene magnetostratigraphy, biostratigraphy, and paleogeography – calcareous nannofossil evidence. Geology 13, 198–202.

Berggren, W.A., Kent, D.V., Aubry, M.-P., Hardenbol, J. (Eds.), 1995. Chronology, Timescales and Global Stratigraphic Correlation. SEPM Spec. Publ. 54, Tulsa, AR, 386 pp.

Bigg, P.J., 1982. Eocene planktonic foraminifera and calcareous nannoplankton from the southern Aquitaine basin, France. Rev. Esp. Micropaleontol. 13, 367–400.

Brinkhuis, H., Biffi, U., 1993. Dinoflagellate cyst stratigraphy of the Eocene–Oligocene transition in central Italy. Mar. Micropaleontol. 22, 131–183.

Brinkhuis, H., 1994. Late Eocene to Early Oligocene dinoflagellate cysts from the Priabonian type-area (Northeast Italy) – biostratigraphy and paleoenvironmental interpretation. Palaeogeogr. Palaeoclimatol. Palaeoecol. 107, 121–163.

Brinkhuis, H., Visscher, H., 1995. The upper boundary of the Priabonian Stage: A reappraisal based on dinoflagellate cyst biostratigraphy. In: Berggren, W.A., Kent, D.V., Aubry, M.-P., Hardenbol, J. (Eds.), Geochronology, Timescales and Global Stratigraphic Correlation. SEPM Spec. Publ. 54, 295–304.

Brown, S., Downie, C., 1984. Dinoflagellate cyst biostratigraphy of late Paleocene and early Eocene sediments from holes 552, 553A and 555, Leg 81, Deep Sea Drilling Project (Rockall Plateau). In: Roberts, D.G., Schnitker, D., Backman, J., Baldauf, J.G., Desprairies, A., Homrighausen, R., Huddlestun, P., Kallenback, A.J., Krumsiek, K.A.O., Morton, A.C., Murray, J.W., Westberg-Smith, J., Zimmerman, H.B. (Eds.), Init. Rep. DSDP 81, 565–579.

Bujak, J.P., 1979. Proposed phylogeny of the dinoflagellates *Rhombodinium* and *Gochtodinium*. Micropaleontology 25, 308–324.

Bujak, J.P., 1980. Dinoflagellate cysts and acritarchs from the Eocene Barton Beds of southern England. In: Bujak, J.P., Downie, C., Eaton, G.L., Williams, G.L. (Eds.), Dinoflagellate Cysts and Acritarchs from the Eocene of Southern England. Spec. Pap. Palaeontol., Palaeontol. Assoc., London, 36–91.

Bujak, J.P., 1994. New dinocyst taxa from the Eocene of the North Sea. J. Micropalaeontol. 13, 119–131.

Bujak, J.P., Mudge, D., 1994. A high-resolution North Sea Eocene dinocyst zonation. J. Geol. Soc. Lond. 151, 449–462.

Cande, S.C., Kent, D.V., 1992. A new geomagnetic polarity time scale for the Late Cretaceous and Cenozoic. J. Geophys. Res. 97, 13917–13951.

Cande, S.C., Kent, D.V., 1995. Revised calibration of the geomagnetic polarity timescale for the Late Cretaceous and Cenozoic. J. Geophys. Res. 100, 6093–6095.

Carney, J.L., Pierce, R.W., 1995. Graphic correlation and composite standard databases as tools for the exploration biostratigrapher. SEPM Spec. Publ. 53, 23–43.

Cepek, P., Köthe, A., Muller, C., 1988. The regional distribution of nannoplankton assemblages; correlation of the interregional zonation with the lithostratigraphic formations. The Federal Republic of Germany, Lower Saxony, Schleswig-Holstein. In: Vinken, R.C. (Ed.), The Northwest European Tertiary Basin. Results of the International Geological Correlation Programme, Project No. 124. Geol. Jb. Reihe A. 100, 275–279.

Costa, L.I., Downie, C., 1976. The distribution of the dinoflagellate *Wetzeliella* in the Palaeogene of northwestern Europe. Palaeontology 19, 591–614.

Costa, L.I., Manum, S.B., Meyer, K.-J., 1988. The regional distribution of dinoflagellates; correlation of the interregional zonation with the local zones and regional lithostratigraphy. Great Britain/Norway. The Viking Graben. In: Vinken, R.C. (Ed.), The Northwest European Tertiary Basin. Results of the International Geological Correlation Programme, Project No. 124. Geol. Jb. Reihe A. 100, 330–332.

Dale, B., 1996. Dinoflagellate cyst ecology: modelling and geological applications. In: Jansonius, J., McGregor, D.C. (Eds.), Palynology: Principles and Applications, vol. 3. AASP Found., pp. 1249–1275.

Damassa, S.P., Goodman, D.K., Kidson, E.J., Williams, G.L., 1990. Correlation of Paleogene dinoflagellate assemblages to standard nannofossil zonation in North-Atlantic DSDP sites. Rev. Palaeobot. Palynol. 65, 331–339.

Damassa, S.P., Williams, G.L., 1996. Species diversity patterns in North Atlantic Eocene–Oligocene dinoflagellates. In: Moguilevsky, A., Whatley, R. (Eds.), Microfossils and Oceanic Environments. University of Wales, Aberystwyth-Press, Aberystwyth, pp. 187–203.

De Coninck, J., 1977. Organic walled phytoplankton from the Eocene of the Woensdrecht borehole, southern Netherlands. Meded. Rijks Geol. Dienst 28, 33–64.

De Coninck, J., 1986. Organic walled phytoplankton from the Bartonian and Eo-Oligocene transitional deposits of the Woensdrecht borehole, southern Netherlands. Meded. Rijks Geol. Dienst 40, 1–49.

Dowsett, H.J., 1989. Application of the graphic correlation method to Pliocene marine sequences. Mar. Micropaleontol. 14, 3–32.

Eaton, G.L., 1976. Dinoflagellate cysts from the Bracklesham beds (Eocene) of the Isle of Wight, Southern England. Bull. Br. Mus. Nat. Hist. Geol. 26, 332 pp.

Edwards, L.E., 1984. Insights on why graphic correlation (Shaw method) works. J. Geol. 92, 583–597.

Eldholm, O., Myhre, A.M., Thiede, J., 1994. Cenozoic tectono-magmatic events in the North Atlantic: Potential palaeoenvironmental implications. In: Boulter, M.C., Fisher, H.C. (Eds.), Cenozoic Plants and Climates of the Arctic. NATO ASI Series 127, Springer, Berlin, pp. 35–55.

Eldholm, O., Thiede, J., Taylor, E., Barton, C., Bjørklund, K., Bleil, U., Ciesielski, P., Desprairies, A., Donnally, D., Froget, C., Goll, R., Henrich, R., Jansen, E., Krissek, L., Kvenvolden, K., LeHurray, A., Love, D., Lysne, P., McDonald, T., Mudie, P., Osterman, L., Parson, L., Phillips, J.D., Pittenger, A., Qvale, G., Schönharting, G., Viereck, L., 1987. Proc. ODP, Init. Rep. 104. Ocean Drilling Program, College Station, TX, 783 pp.

Firth, J.V., 1996. Upper middle Eocene to Oligocene dinoflagellate biostratigraphy and assemblage variations in Hole 913B, Greenland Sea. In: Myhre, A.M., Thiede, J., Firth, J.V., Johnson, G.L., Ruddiman, W.F. (Eds.), Proc. ODP, Sci. Results 151. Ocean Drilling Program, College Station, TX, pp. 203–242.

Fisher, O., 1862. On the Bracklesham Beds of the Isle of Wight Basin. Quart. J. Geol. Soc. Lond. 18, 65–94.

Fuller, M., Hastedt, M., Herr B., 1998. Coring-induced magnetization of recovered sediment. In: Weaver, P.P.E., Schmincke, H.-U., Firth, J.V., Duffield, W. (Eds.), Proc. ODP, Sci. Results 157. Ocean Drilling Program, College Station, TX, pp. 47–56.

Goll, R.M., 1989. A synthesis of Norwegian–Greenland Sea biostratigraphies: ODP Leg 104 on the Vøring Plateau. In: Eldholm, O., Thiede, J., Taylor, E., Barton, C., Bjørklund, K., Bleil, U., Ciesielski, P., Desprairies, A., Donnally, D., Froget, C., Goll, R., Henrich, R., Jansen, E., Krissek, L., Kvenvolden, K., Letturay, A., Love, D., Lynse, P., McDonald, T., Mudie, P., Osterman, L., Parson, L., Phillips, J.D., Pittenger, A., Qvale, G., Schönharting, G., Viereck, L. (Eds.), Proc. ODP, Sci. Results 104. Ocean Drilling Program, College Station, TX, pp. 777–826.

Florindo, F., Roberts, A.P., Palmer, M.R., 2003. Magnetite dissolution in siliceous sediments, Geochem. Geophys. Geosyst. 4, doi: 10.1029/2003GC000516.

Gradstein, F.M., Kristiansen, I.L., Loemo, L., Kaminski, M.A., 1992. Cenozoic foraminiferal and dinoflagellate biostratigraphy of the Central North Sea. Micropaleontology 38, 101–137.

Harland, R., Hine, N.M., Wilkinson, I.P., 1992. Paleogene biostratigraphic markers. In: Knox, R.W.O.B., Holloway, S. (Eds.), Paleogene of the Central and Northern North Sea. Brit. Geol. Surv. Nottingham, pp. A1–A5.

Head, M.J., Norris, G., 1989. Palynology and dinocyst stratigraphy of the Eocene and Oligocene in ODP Leg 105, Hole 647A, Labrador Sea. In: Srivastava, S.P., Arthur, M.A., Clement, B. (Eds.), Proc. ODP, Sci. Results 105. Ocean Drilling Program, College Station, TX, pp. 515–550.

Heilmann-Clausen, C., Costa, L.I., 1989. Dinoflagellate zonation of the uppermost Paleocene? to Lower Miocene in the Wursterheide research well, NW Germany. Geol. Jb. Reihe A. 111, 431–521.

Ioakim, C., 1979. Étude comparative des dinoflagellés du Tertiaire inférieur de la Mer du Labrador et de la Mer du Nord. Thèse de troisième cycle, Université Pierre et Marie Curie, Paris, 204 pp.

Islam, M.A., 1983. Dinoflagellate cyst taxonomy and biostratigraphy of the Eocene Bracklesham Group in Southern England. Micropaleontology 29, 328–353.

Kapellos, V., Schaub, H., 1975. L'Ilerdien dans les Pyrénéés et en Crimiéé. Corrélation de zones a grands Foraminiferes et a Nannoplancton. Bull. Soc. Géol. Fr. 17, 148–160.

Karlin, R., Levi, S., 1983. Diagenesis of magnetic minerals in Recent haemipelagic sediments. Nature 303, 327–330.

Keller, G., Herbert, T., Dorsey, R., D'Hondt, S., Johnsson, M., Chi, W.R., 1987. Global distribution of late Paleogene hiatuses. Geology 15, 199–203.

Kennett, J.P., 1977. Cenozoic evolution of Antarctic glaciation, the Circum-Antarctic Ocean, and their impact on global paleoceanography. J. Geophys. Res. 82, 3843–3860.

Kirschvink, J.L., 1980. The least-squares line and plane and the analysis of palaeomagnetic data. Geophys. J. R. Astron. Soc. 62, 699–718.

Köthe, A., 1990. Paleogene dinoflagellates from Northwest Germany – biostratigraphy and palaeoenvironment. Geol. Jb. Reihe A 118, 111 pp.

Manum, S.B., 1960. Some dinoflagellates and hystrichosphaerids from the Lower Tertiary of Spitsbergen. Nytt Mag. Bot. 8, 17–26.

Manum, S.B., 1976. Dinocysts in Tertiary Norwegian–Greenland Sea sediments (Deep Sea Drilling Project 38), with observations on palynomorphs and palynodebris in relation to environment. In: Talwani, M., Udinstev, G., Bjørklund, K., Caston, V.N.D., Faas, R.W., Kharin, G.N., Morris, D.A. (Eds.), Init. Rep. DSDP 38. US Gov. Print. Off., Washington, DC, pp. 897–919.

Manum, S.B., Throndsen, T., 1986. Age of Tertiary formations on Spitsbergen. Polar Res. 4, 103–131.

Manum, S.B., Boulter, M.C., Gunnarsdottir, H., Rangnes, K., Scholze, A., 1989. Eocene to Miocene palynology of the Norwegian–Greenland Sea (ODP Leg 104). In: Eldholm, O., Thiede, J., Taylor, E., Barton, C., Bjørklund, K., Bleil, U., Ciesielski, P., Desprairies, A., Donnally, D., Froget, C., Goll, R., Henrich, R., Jansen, E., Krissek, L., Kvenvolden, K., Letturay, A., Love, D., Lynse, P., McDonald, T., Mudie, P., Osterman, L., Parson, L., Phillips, J.D., Pittenger, A., Qvale, G., Schönharting, G., Viereck, L. (Eds.), Proc. ODP, Sci. Results 104. Ocean Drilling Program, College Station, TX, pp. 611–662.

Michoux, D., 1988. Dinoflagellate cysts of the *Wetzeliella*-complex from Eocene sediments of the Aquitaine Basin, southwestern France. Palynology 12, 11–41.

Miller, F.X., 1977. The graphic correlation method in biostratigraphy. In: Kauffman, E., Hazel, J. (Eds.), Concepts and Methods of Biostratigraphy. Dowden, Hutchinson and Ross, Stroudsburg, pp. 165–186.

Miller, K.G., 1992. Middle Eocene to Oligocene stable iso-

topes, climate, and deep-water history: The terminal Eocene event? In: Prothero, D.R., Berggren, W.A. (Eds.), Eocene–Oligocene Climatic and Biotic Evolution. Princeton University Press, Princeton, pp. 160–177.

Miller, K.G., Fairbanks, R.G., Mountain, G.S., 1987. Tertiary oxygen isotope synthesis, sea level history, and continental margin erosion. Paleoceanography 2, 1–19.

Molina, E., Gonzalvo, C., Keller, G., 1993. The Eocene–Oligocene planktic foraminiferal transition – extinctions, impacts and hiatuses. Geol. Mag. 130, 483–499.

Mudge, D.C., Bujak, J.P., 1996. An integrated stratigraphy for the Paleocene and Eocene of the North Sea. In: Knox, R.W.O.B., Corfield, R.M., Dunay, R.E. (Eds.), Correlation of the Early Paleogene in Northwest Europe. Geol. Soc. Spec. Publ. 101, 91–113.

Myhre, A.M., Thiede, J., Firth, J.V., Ahagon, N., Chow, N., Cremer, M., Davis, L., Flower, B., Fronval, T., 1995. Proc. ODP, Init. Rep. 151. Ocean Drilling Program, College Station, TX, 926 pp.

Neal, J.E., Stein, J.A., Gamber, J.H., 1994. Graphic correlation and sequence stratigraphy in the Palaeogene of NW Europe. J. Micropalaeontol. 13, 55–80.

Poulsen, N.E., Manum, S.B., Williams, G.L., Ellegaard, M., 1996. Tertiary dinoflagellate biostratigraphy of sites 907, 908 and 909 in the Norwegian–Greenland Sea. In: Thiede, J., Myhre, A.M., Firth, J.V., Johnson, G.L., Ruddiman, W.F. (Eds.), Proc. ODP, Sci. Results 151. Ocean Drilling Program, College Station, TX, pp. 255–287.

Powell, A.J., 1992. Dinoflagellate cysts of the Tertiary System. In: Powell, A.J. (Ed.), A Stratigraphic Index of Dinoflagellate Cysts. Chapman and Hall, London, pp. 155–251.

Prentice, M.L., Matthews, R.K., 1988. Cenozoic ice-volume history – development of a composite oxygen isotope record. Geology 16, 963–966.

Roberts, A.P., Stoner, J.S., Richter, C., Coring-induced magnetic overprints and limitations of the long-core paleomagnetic measurement technique: some observations from ODP Leg 160, Eastern Mediterranean Sea. In: Emeis, K-C., Robertson, A.H.F., Richter, C., Blanc-Valleron, M-M., Bouloubassi, I., Brumsack, H-J., Cramp, A., De Lange, G.J., Di Stefano, E., Flecker, R., Frankel, E., Howell, M.W., Janecek, T.R., Jurado-Rodriguez, M-J., Kemp, A.E.S., Koizumi, I., Kopf, A., Major, C.O., Mart, Y., Pribnow, D.F.C., Rabaute, A., Roberts, A.P., Rullköter, J.H., Sakamoto, T., Spezzaferri, S., Staerker, T.S., Stoner, J.S., Whiting, B.M., Woodside, J.M. (Eds.), Proc. ODP, Init. Rep. 160. Ocean Drilling Program, College Station, TX, pp. 497–505.

Schrader, H., Bjørklund, K., Manum, S.B., Martini, E., von Hinte, J., 1976. Cenozoic biostratigraphy, physical stratigraphy and paleoceanography in the Norwegian–Greenland Sea, DSDP Leg 38, paleontological synthesis. In: Talwani, M., Udinstev, G., Bjørklund, K., Caston, V.N.D., Faas, R.W., Kharin, G.N., Morris, D.A. (Eds.), Init. Rep. DSDP 38. US Gov. Print. Off., Washington, DC, pp. 1197–1213.

Shackleton, N.J., Kennett, J.P., 1975. Paleotemperature history of the Cenozoic and the initiation of Antarctic glaciation: Oxygen and carbon isotope analysis in DSDP sites 277, 279 and 281. In: Kennett, J.P., Houtz, R.E., Andrews, P.B., Edwards, A.R., Gostin, V.A., Hajós, M., Hampton, M.A., Jenkins, D.G., Margolis, S.V., Ovenshine, T., Perch-Nielsen, T., (Eds.), Init. Rep. DSDP 29. US Gov. Print. Off., Washington, DC, pp. 743–756.

Shaw, A.B., 1964. Time in Stratigraphy. McGraw Hill Brook, New York, 365 pp.

Skogseid, J., Eldholm, O., 1989. Vøring Plateau continental margin: seismic interpretation, stratigraphy and vertical movements. In: Eldholm, O., Thiede, J., Taylor, E., Barton, C., Bjørklund, K., Bleil, U., Ciesielski, P., Desprairies, A., Donnally, D., Froget, C., Goll, R., Henrich, R., Jansen, E., Krissek, L., Kvenvolden, K., Letturay, A., Love, D., Lynse, P., McDonald, T., Mudie, P., Osterman, L., Parson, L., Phillips, J.D., Pittenger, A., Qvale, G., Schönharting, G., Viereck, L. (Eds.), Proc. ODP, Sci. Results 104. Ocean Drilling Program, College Station, TX, pp. 993–1032.

Stockmarr, J., 1971. Tablets with spores used in absolute pollen analysis. Pollen Spores 13, 615–621.

Stover, L.E., Hardenbol, J., 1994. Dinoflagellates and depositional sequences in the Lower Oligocene (Rupelian) Boom Clay Formation, Belgium. Bull. Soc. Belg. Géol. 102, 5–77.

Stover, L.E., Williams, G.L., 1995. A revision of the Paleogene dinoflagellate genera *Areosphaeridium* Eaton 1971 and *Eatonicysta* Stover and Evitt 1978. Micropaleontology 41, 97–141.

Stover, L.E., Williams, G.L., Eaton, G.L., 1988. Morphology and stratigraphy of the Paleogene dinoflagellate genus *Areosphaeridium* Eaton, 1971. Proc. 7th Int. Palynol. Conf., Brisbane (Abstracts), p. 157.

Talwani, M., Udinstev, G., Bjørklund, K., Caston, V.N.D., Faas, R.W., Kharin, G.N., Morris, D.A., 1976. Init. Rep. DSDP 38. US Gov. Print. Off., Washington, DC.

Thiede, J., Myhre, A.M., 1996. The paleoceanographic history of the North Atlantic–Arctic gateways: synthesis of Leg 151 drilling results. In: Thiede, J., Myhre, A.M., Firth, J.V., Johnson, G.L., Ruddiman, W.F. (Eds.), Proc. ODP, Sci. Results 151. Ocean Drilling Program, College Station, TX, pp. 645–659.

Verbeek, J.W., 1988. The regional distribution of nannoplankton assemblages; correlation of the interregional zonation with the regional lithostratigraphic formations. The Netherlands. In: Vinken, R.C. (Ed.), The Northwest Tertiary Basin. Results of the International Geological Correlation Programme, Project No. 124. Geol. Jb. Reihe A. 100, 273–275.

Verbeek, J.W., Steurbaut, E., Moorkens, T., 1988. The regional distribution of nannoplankton assemblages; correlation of the interregional zonation with the regional lithostratigraphic formations. Belgium. In: Vinken, R.C. (Ed.), The Northwest Tertiary Basin. Results of the International Geological Correlation Programme, Project No. 124. Geol. Jb. Reihe A. 100, 267–273.

Williams, G.L., 1975. Dinoflagellate and spore stratigraphy of the Mesozoic–Cenozoic, offshore eastern Canada. Geol. Surv. Can. Pap. 2, 107–161.

Williams, G.L., 1977. Dinoflagellates: their palaeontology,

biostratigraphy and palaeoecology. In: Ramsay, A.T.S. (Ed.), Oceanic Micropalaeontology. London, pp. 1231–1325.

Williams, G.L., Bujak, J.P., 1985. Mesozoic and Cenozoic dinoflagellates. In: Bolli, H.M., Saunders, J.B., Perch-Nielsen, K. (Eds.), Plankton Stratigraphy. Cambridge University Press, Cambridge, pp. 847–964.

Williams, G.L., Fensome, R.E., Bujak, J.P., Brinkhuis, H., 1999. Mesozoic–Cenozoic Dinoflagellate Cyst Course. LPP, Urbino (unpublished).

Williams, G.L., Stover, L.E., Kidson, E.J., 1993. Morphology and stratigraphic ranges of selected Mesozoic–Cenozoic dinoflagellate taxa in the Northern Hemisphere. Geol. Surv. Can. Pap. 92–10, 137 pp.

Williams, G.L., Lentin, J.K., Fensome, R.A. (Eds.), 1998. The Lentin and Williams index of fossil dinoflagellates, 1998 edition. AASP Contrib. Ser. 34, 744 pp.

Williams, G.L., Manum, S.B., 1999. Oligocene–early Miocene dinocyst stratigraphy of Hole 985A, Norwegian Sea. In: Raymo, M.E., Jansen, E., Blum, P., Herbert, T.D. (Eds.), Proc. ODP 162. Ocean Drilling Program, College Station, TX, pp. 99–109.

Williams, G.L., Boessenkool, K.P., Brinkhuis, H., Pearce, M.A., 2001. Upper Cretaceous–Neogene Dinoflagellate Cyst Course morphology, stratigraphy and paleoecology. LPP, Urbino (unpublished).

Zachos, J.C., Stott, L.D., Lohmann, K.C., 1994. Evolution of early Cenozoic marine temperatures. Paleoceanography 9, 353–387.

Zachos, J., Pagani, M., Sloan, L., Thomas, E., Billups, K., 2001. Trends, rhythms, and aberrations in global climate 65 Ma to present. Science 292, 686–693.